EUROPEAN ORGANIZATION FOR NUCLEAR RESEARCH

CERN-EP-2020-186
1 October 2020

Production of muons from heavy−flavour hadron decays at high transverse momentum in Pb−Pb collisions at $\sqrt{s_{\mathrm{NN}}} = 5.02$ and 2.76 TeV

ALICE Collaboration*

Abstract

Measurements of the production of muons from heavy-flavour hadron decays in Pb–Pb collisions at $\sqrt{s_{\mathrm{NN}}} = 5.02$ and 2.76 TeV using the ALICE detector at the LHC are reported. The nuclear modification factor R_{AA} at $\sqrt{s_{\mathrm{NN}}} = 5.02$ TeV is measured at forward rapidity ($2.5 < y < 4$) as a function of transverse momentum p_{T} in central, semi-central, and peripheral collisions over a wide p_{T} interval, $3 < p_{\mathrm{T}} < 20$ GeV/c, in which a significant contribution of muons from beauty-hadron decays is expected at high p_{T}. With a significantly improved precision compared to the measurements at lower collision energy, the R_{AA} shows an increase of the suppression of the yields of muons from heavy-flavour hadron decays with increasing centrality. A suppression by a factor of about three is observed in the 10% most central collisions. The R_{AA} at $\sqrt{s_{\mathrm{NN}}} = 5.02$ TeV is similar to that reported at $\sqrt{s_{\mathrm{NN}}} = 2.76$ TeV in a broader p_{T} interval and with an improved accuracy with respect to previously published measurements. The precise R_{AA} results have the potential to distinguish between model predictions implementing different mechanisms of parton energy loss in the high-density medium formed in heavy-ion collisions. The results place stringent constraints on the relative energy loss between charm and beauty quarks.

---

[*] See Appendix A for the list of collaboration members

1 Introduction

The study of ultra-relativistic heavy-ion collisions aims to investigate a state of strongly-interacting matter at high energy density and temperature. Under these extreme conditions, quantum chromodynamics (QCD) calculations on the lattice predict the formation of a quark–gluon plasma (QGP), where quarks and gluons are deconfined, and chiral symmetry is partially restored [1–4].

Heavy quarks (charm and beauty) are key probes of the QGP properties in the laboratory. They are predominantly created in hard-scattering processes at the early stage of the collision on a timescale shorter than the formation time of the QGP of ~ 0.1–1 fm/c [5, 6]. Therefore, they experience the full evolution of the hot and dense QCD medium. During their propagation through the medium, they lose energy via radiative and collisional processes [7–12]. Quarks are expected to lose less energy than gluons due to the colour-charge dependence of the strong interaction. Furthermore, several mass-dependent effects can also influence the energy loss. Due to the dead-cone effect [8, 9, 13], the heavy-quark radiative energy loss is reduced compared to that of light quarks and the energy loss of beauty quarks is expected to be smaller than that of charm quarks. The collisional heavy-quark energy loss is also expected to be reduced since the spatial diffusion coefficient, which controls the momentum exchange with the medium, is predicted to scale with the inverse of the quark mass [14]. In addition to the heavy-quark energy loss, modifications of the hadronisation process via fragmentation and/or recombination [15, 16] and initial-state effects such as the modification of the parton distribution functions (PDF) inside the nucleus [17–19] can also change the particle yields and phase-space distributions. The medium effects can be quantified using the nuclear modification factor R_{AA}, which is the ratio between the p_{T}- and y-differential particle yields in nucleus-nucleus (AA) collisions ($\mathrm{d}^2N_{\mathrm{AA}}/\mathrm{d}p_{\mathrm{T}}\mathrm{d}y$) and the corresponding production cross section in pp collisions ($\mathrm{d}^2\sigma_{\mathrm{pp}}/\mathrm{d}p_{\mathrm{T}}\mathrm{d}y$) scaled by the average nuclear overlap function $\langle T_{\mathrm{AA}}\rangle$:

$$R_{\mathrm{AA}}(p_{\mathrm{T}},y) = \frac{1}{\langle T_{\mathrm{AA}}\rangle} \times \frac{\mathrm{d}^2N_{\mathrm{AA}}/\mathrm{d}p_{\mathrm{T}}\mathrm{d}y}{\mathrm{d}^2\sigma_{\mathrm{pp}}/\mathrm{d}p_{\mathrm{T}}\mathrm{d}y}. \tag{1}$$

The $\langle T_{\mathrm{AA}}\rangle$ is defined as the ratio between the average number of nucleon–nucleon collisions $\langle N_{\mathrm{coll}}\rangle$ and the inelastic nucleon–nucleon cross section [20].

Evidence of a strong suppression of open heavy-flavour yields was observed in central Au–Au and Cu–Cu collisions at $\sqrt{s_{\mathrm{NN}}} = 200$ GeV by the PHENIX and STAR collaborations at RHIC and in Pb–Pb collisions at $\sqrt{s_{\mathrm{NN}}} = 2.76$ TeV by the ALICE, ATLAS, and CMS collaborations at the LHC (see [5] and references therein, and [21–24]). Recently, the ALICE and CMS collaborations reported a significant suppression of the D-meson yields measured at midrapidity in the 10% most central Pb–Pb collisions at $\sqrt{s_{\mathrm{NN}}} = 5.02$ TeV with respect to the scaled pp reference, reaching a factor of about 5–6 in the interval $8 < p_{\mathrm{T}} < 12$ GeV/c [25, 26]. A strong suppression of the yields of high-p_{T} electrons from heavy-flavour hadron decays was also observed by the ALICE collaboration at midrapidity in the 0–10% centrality class, where the measured R_{AA} is about 0.3 at $p_{\mathrm{T}} \sim 7$ GeV/c [24]. The suppression is similar to that observed for D mesons and leptons from heavy-flavour hadron decays at $\sqrt{s_{\mathrm{NN}}} = 2.76$ TeV [21, 27, 28]. The nuclear modification factor of $\mathrm{B}^{\pm}$ mesons, reconstructed via the exclusive decay channel $\mathrm{B}^{\pm} \to \mathrm{J}/\psi\mathrm{K}^{\pm} \to \mu^{+}\mu^{-}\mathrm{K}^{\pm}$ with the CMS detector for $|y| < 2.4$ and $7 < p_{\mathrm{T}} < 50$ GeV/c, indicates a suppression of about a factor two in Pb–Pb collisions (0–100% centrality class) at $\sqrt{s_{\mathrm{NN}}} = 5.02$ TeV [29] compatible with that of non-prompt J/ψ [30]. A similar suppression as for $\mathrm{B}^{\pm}$ mesons and non-prompt J/ψ is also observed for non-prompt D^0 mesons in the kinematic region $|y| < 2.4$ and $2 < p_{\mathrm{T}} < 100$ GeV/c [31]. The suppression of B mesons is weaker than that of prompt D^0 mesons at about $p_{\mathrm{T}} = 10$ GeV/c, in line with the expected quark-mass ordering of energy loss.

Complementary measurements of the muons from heavy-flavour hadron decays in the forward rapidity region ($2.5 < y < 4.0$), presently only covered by ALICE in Pb–Pb collisions, are discussed in this paper. Such measurements profit from muon triggers and large branching ratios ($\sim 10\%$). Consequently, differential measurements are carried out over a wide p_{T} interval.

This letter presents the first measurement of the open heavy-flavour production via muons from semi-leptonic decays of charm and beauty hadrons at forward rapidity ($2.5 < y < 4$) in Pb–Pb collisions at $\sqrt{s_{\rm NN}} = 5.02$ TeV with the ALICE detector at the LHC. High precision measurements of the $p_{\rm T}$-differential $R_{\rm AA}$ of these muons over a broad $p_{\rm T}$ interval, extended for the first time to $p_{\rm T} = 20$ GeV/c in centrality classes from 0 to 80% are presented. This gives access to the investigation of medium effects in a new kinematic regime where the contribution of muons originating from B hadrons is dominant at high $p_{\rm T}$. New measurements in central Pb–Pb collisions at $\sqrt{s_{\rm NN}} = 2.76$ TeV, with a significantly extended $p_{\rm T}$ coverage and a higher precision compared to the previous ALICE publication [32], are reported and compared to the results at $\sqrt{s_{\rm NN}} = 5.02$ TeV. Detailed comparisons with model calculations with different implementations of in-medium energy loss are discussed as well.

2 Experimental apparatus and data samples

The ALICE apparatus and its performance are described in [33, 34]. The analysis is based on the detection of muons in the forward muon spectrometer covering the pseudorapidity interval $-4 < \eta < -2.5$[1]. The muon spectrometer consists of a front absorber of 10 nuclear interaction lengths ($\lambda_{\rm I}$) filtering hadrons, followed by five tracking stations, each composed of two planes of Cathode Pad Chambers, with the third station inside a dipole magnet with a field integral of 3 T×m. The tracking system is complemented with two trigger stations, each equipped with two planes of Resistive Plate Chambers downstream an iron wall of 7 $\lambda_{\rm I}$. Finally, a conical absorber shields the muon spectrometer against secondary particles produced by the interaction of primary particles at large η in the beam pipe. The Silicon Pixel Detector (SPD), made of two cylindrical layers covering the pseudorapidity intervals $|\eta| < 2$ and $|\eta| < 1.4$, is employed for the reconstruction of the primary vertex. Two V0-scintillator arrays covering $2.8 < \eta < 5.1$ and $-3.7 < \eta < -1.7$ provide a minimum bias (MB) trigger defined as the coincidence of signals from the two hodoscopes. The V0 detectors are also used to classify events according to their centrality, determined from a fit of the total signal amplitude based on a two-component particle production model connected to the collision geometry using the Glauber formalism [35]. The centrality intervals are defined as percentiles of the Pb–Pb hadronic cross section. The V0 and the Zero Degree Calorimeters (ZDC), placed at ±112.5 m from the interaction point along the beam direction, are used for the event selection.

The results presented in this letter are based on the data sample recorded with the ALICE detector during the 2015 Pb–Pb run at a centre-of-mass energy $\sqrt{s_{\rm NN}} = 5.02$ TeV. For the comparison with measurements at lower energy, $\sqrt{s_{\rm NN}} = 2.76$ TeV, the 2011 data sample is used in order to extend the $p_{\rm T}$ coverage with respect to the published results from the 2010 data sample [32]. The analysis of the two data samples is based on muon-triggered events requiring a MB trigger and at least one track segment in the muon trigger system with a $p_{\rm T}$ larger than a programmable threshold [33]. Data were collected with two $p_{\rm T}$-trigger thresholds of about 1 and 4.2 GeV/c at $\sqrt{s_{\rm NN}} = 5.02$ TeV, and of about 0.5 and 4.2 GeV/c at $\sqrt{s_{\rm NN}} = 2.76$ TeV. The $p_{\rm T}$ threshold of the trigger algorithm is set such that the corresponding efficiency for muon tracks is 50%. In the following, the low- and high-$p_{\rm T}$ trigger-threshold samples are referred to as MSL and MSH, respectively. The beam-induced background is reduced offline using the V0 and ZDC timing information, and electromagnetic interactions are removed by requiring a minimum energy deposited in the ZDC. Only events with a primary vertex within ±10 cm along the beam line are analysed. Finally, the analyses are limited to the 80% most central collisions. After the event selection, the data samples correspond to integrated luminosities of about 21.9 (224.8) μb^{-1} and 4.0 (71.0) μb^{-1} for MSL- (MSH-) triggered events at $\sqrt{s_{\rm NN}} = 5.02$ and 2.76 TeV, respectively. The integrated luminosity is derived from the number of muon-triggered events. The latter is normalised by a factor, inversely proportional to the probability of having a muon trigger in a MB event in a given centrality class, calcu-

---

[1] The muon spectrometer covers a negative η range in the ALICE reference frame and consequently a negative y range. The results are chosen to be presented with a positive y notation, due to the symmetry of the collision system.

lated by applying the muon-trigger condition in the analysis of MB events or from the relative count rate of the two triggers.

3 Analysis procedure

Standard selection criteria are applied to the muon candidates [36]. Tracks in the muon spectrometer are reconstructed within the pseudorapidity range $-4 < \eta < -2.5$ and they are required to have a polar angle measured at the exit of the absorber in the interval $170^\circ < \theta_{\rm abs} < 178^\circ$. Furthermore, tracks are identified as muons if they match a track segment in the trigger system. Finally, the remaining beam-induced background is reduced by requiring the distance of the track to the primary vertex measured in the transverse plane (DCA, distance of closest approach) weighted with its momentum (p), $p \times$ DCA, to be smaller than $6 \times \sigma_{p\rm DCA}$, with $\sigma_{p\rm DCA}$ being the width of the distribution.

The nuclear modification factor $R_{\rm AA}$ of muons from heavy-flavour hadron decays is measured down to $p_{\rm T} = 3$ GeV/c and up to $p_{\rm T} = 20$ GeV/c in the three centrality classes 0–10%, 20–40% and 60–80% at $\sqrt{s_{\rm NN}} = 5.02$ TeV and in the 0–10% centrality class at $\sqrt{s_{\rm NN}} = 2.76$ TeV. These measurements are performed by using MSL-triggered events up to $p_{\rm T} = 7$ GeV/c and MSH-triggered events at $p_{\rm T} > 7$ GeV/c. In the selected $p_{\rm T}$ interval, the remaining background contributions to the muon yields consist of muons from primary charged-pion and kaon decays and muons from W-boson, Z-boson, and γ^* (Drell-Yan process) decays which are the main background sources at $p_{\rm T} < 6$ GeV/c and $p_{\rm T} > 13$ GeV/c, respectively. The two small contributions of muons from secondary (charged) light-hadron decays in the interval $3 < p_{\rm T} < 5$ GeV/c, resulting from the interaction of light hadrons with the material of the front absorber and of muons from J/ψ decays over the entire $p_{\rm T}$ range, are also considered. Therefore, the $p_{\rm T}$-differential $R_{\rm AA}$ of muons from heavy-flavour hadron decays in a given centrality class is expressed as

$$R_{\rm AA}(p_{\rm T},y) = \frac{\left(\dfrac{{\rm d}^2N^{\mu^\pm}}{{\rm d}p_{\rm T}{\rm d}y} - \displaystyle\sum_{\text{non-HF}\to\mu^\pm} \dfrac{{\rm d}^2N^{\text{non-HF}\to\mu^\pm}}{{\rm d}p_{\rm T}{\rm d}y}\right)_{\rm Pb--Pb}}{\langle T_{\rm AA}\rangle \times \left(\dfrac{{\rm d}^2\sigma^{\rm c,b\to\mu^\pm}}{{\rm d}p_{\rm T}{\rm d}y}\right)_{\rm pp}}, \tag{2}$$

where ${\rm d}^2N^{\mu^\pm}/{\rm d}p_{\rm T}{\rm d}y$ is the differential yield of inclusive muons and $\sum_{\text{non-HF}\to\mu^\pm} {\rm d}^2N^{\text{non-HF}\to\mu^\pm}/{\rm d}p_{\rm T}{\rm d}y$ refers to the differential yields of muons from various non heavy-flavour sources in Pb–Pb collisions, as indicated above Eq. (2). In the denominator, ${\rm d}^2\sigma^{\rm c,b\to\mu^\pm}/{\rm d}p_{\rm T}{\rm d}y$ is the pp differential production cross section of muons from heavy-flavour hadron decays at the same centre-of-mass energy and in the same kinematic region (see [32, 36]) as in Pb–Pb collisions.

The inclusive muon yields in Pb–Pb collisions at $\sqrt{s_{\rm NN}} = 5.02$ TeV are corrected for detector acceptance and detection efficiencies ($A \times \varepsilon$) using the procedure described in previous publications [32, 36]. In peripheral collisions, $A \times \varepsilon$ amounts to about 90% with almost no $p_{\rm T}$ dependence in the region of interest for MSL-triggered events, while for MSH-triggered events the $A \times \varepsilon$ increases with $p_{\rm T}$ with a saturation at a value close to 90% for $p_{\rm T} > 14$ GeV/c. The dependence of the trigger and tracking efficiency on the detector occupancy is determined by embedding simulated muons from heavy-flavour hadron decays in measured MB Pb–Pb events. A decrease in the efficiency of 6% from peripheral (60–80%) to central (0–10%) collisions, independent of $p_{\rm T}$ is observed.

The estimation of the contribution of muons from primary $\pi^\pm$ and $\rm K^\pm$ decays is based on a data-tuned Monte Carlo cocktail. The procedure uses the midrapidity ($|\eta| < 0.8$) $\pi^\pm$ and $\rm K^\pm$ spectra measured by the ALICE collaboration up to $p_{\rm T} = 20$ GeV/c [37] in pp and Pb–Pb collisions at $\sqrt{s_{\rm NN}} = 5.02$ TeV. They are further extrapolated to higher $p_{\rm T}$, up to $p_{\rm T} = 40$ GeV/c, by means of a power-law fit to extend the $p_{\rm T}$ coverage to the $p_{\rm T}$ interval relevant for the estimation of the decay muons up to $p_{\rm T} = 20$ GeV/c. Then, the extrapolation to forward rapidities is performed assuming the same suppression of primary $\pi^\pm$

and $\mathrm{K}^{\pm}$ yields from midrapidity up to $y = 4$ according to

$$\left[\frac{\mathrm{d}^2N^{\pi^{\pm}(\mathrm{K}^{\pm})}}{\mathrm{d}p_{\mathrm{T}}\mathrm{d}y}\right]_{\mathrm{AA}} = \langle N_{\mathrm{coll}}\rangle \times \left[R_{\mathrm{AA}}^{\pi^{\pm}(\mathrm{K}^{\pm})}\right]^{\mathrm{mid}-y} \times [F_{\mathrm{extrap}}^{\pi^{\pm}(\mathrm{K}^{\pm})}(p_{\mathrm{T}},y)]_{\mathrm{pp}} \times \left[\frac{\mathrm{d}^2N^{\pi^{\pm}(\mathrm{K}^{\pm})}}{\mathrm{d}p_{\mathrm{T}}\mathrm{d}y}\right]_{\mathrm{pp}}^{\mathrm{mid}-y}. \quad (3)$$

Equation (3) can be also expressed as

$$\left[\frac{\mathrm{d}^2N^{\pi^{\pm}(\mathrm{K}^{\pm})}}{\mathrm{d}p_{\mathrm{T}}\mathrm{d}y}\right]_{\mathrm{AA}} = [F_{\mathrm{extrap}}^{\pi^{\pm}(\mathrm{K}^{\pm})}(p_{\mathrm{T}},y)]_{\mathrm{pp}} \times \left[\frac{\mathrm{d}^2N^{\pi^{\pm}(\mathrm{K}^{\pm})}}{\mathrm{d}p_{\mathrm{T}}\mathrm{d}y}\right]_{\mathrm{AA}}^{\mathrm{mid}-y}, \quad (4)$$

where $[F_{\mathrm{extrap}}^{\pi^{\pm}(\mathrm{K}^{\pm})}(p_{\mathrm{T}},y)]_{\mathrm{pp}}$ is the p_{T}- and y-dependent extrapolation factor in pp collisions at $\sqrt{s} = 5.02$ TeV, discussed in [36], which is based on Monte Carlo simulations. The systematic uncertainty due to the unknown suppression at forward rapidity will be discussed below. The PYTHIA 6.4 [38] and PHOJET [39] event generators are employed for the rapidity extrapolation, while PYTHIA 8.2 simulations [40] with various colour reconnection (CR) options are performed to take into account the rapidity dependence of the p_{T} extrapolation and its uncertainty. The p_{T} and y distributions of muons from primary $\pi^{\pm}$ and $\mathrm{K}^{\pm}$ decays in Pb–Pb collisions are generated according to a fast detector simulation of the decay kinematics and of the effect of the front absorber [36] using as input the extrapolated $\pi^{\pm}$ and $\mathrm{K}^{\pm}$ spectra. For each centrality class, the yields are further subtracted from the inclusive muon distribution. The total contribution of muons from primary $\pi^{\pm}$ and $\mathrm{K}^{\pm}$ decays decreases with increasing p_{T} from about 21% (13%) at $p_{\mathrm{T}} = 3$ GeV/c down to about 7% (4%) at $p_{\mathrm{T}} = 20$ GeV/c in the 60–80% (0–10%) centrality class, with a weak p_{T} dependence for $p_{\mathrm{T}} > 10$ GeV/c.

The estimation of the background of muons from secondary $\pi^{\pm}$ and $\mathrm{K}^{\pm}$ decays produced in the front absorber is based on Monte Carlo simulations using the HIJING event generator [41] and the GEANT3 transport package [42]. These simulation results indicate that in the p_{T} interval of interest, the relative contribution of secondary muons with respect to muons from primary $\pi^{\pm}$ and $\mathrm{K}^{\pm}$ decays is about 9%, independently of both p_{T} and the collision centrality. Given the estimated contamination of muons from primary $\pi^{\pm}$ and $\mathrm{K}^{\pm}$ decays, the contribution of these secondary muons relative to the total muon yield decreases with increasing p_{T} from about 2% (1%) at $p_{\mathrm{T}} = 3$ GeV/c in the 60–80% (0–10%) centrality class to less than 1% at $p_{\mathrm{T}} = 5$ GeV/c for all centrality classes.

The estimation of the contribution of muons from W-boson decays and dimuons from Z-boson and $\gamma^{\star}$ decays, which is relevant in the high-p_{T} region, is based on the POWHEG NLO event generator [43] combined with PYTHIA 6.4.25 [38] for the parton shower which reproduces within uncertainties the W- and Z-boson production in various LHC experiments [44–47]. These calculations include the CT10 PDF set [48] and the EPS09 NLO parameterisation [17] of the nuclear modification of the PDFs. The isospin dependence of the W- and Z/$\gamma^{\star}$-boson production is taken into account. In this regard, pp, np, pn, and nn collisions are simulated separately for both muons from W-boson decays and dimuons from Z-boson decays and $\gamma^{\star}$ decays up to $p_{\mathrm{T}} = 20$ GeV/c. A weighted sum of the production cross sections in the four systems is performed to obtain the production cross section per nucleon–nucleon collision for the Pb–Pb system. The latter is further scaled with $\langle T_{\mathrm{AA}}\rangle$ in a given centrality class in order to estimate the corresponding relative contribution of W and Z/$\gamma^{\star}$ with respect to inclusive muons. The relative contribution of muons from W and Z/$\gamma^{\star}$ with respect to inclusive muons is negligible for $p_{\mathrm{T}} < 13$ GeV/c and it increases with p_{T} and the collision centrality from about 3% (6%) at $p_{\mathrm{T}} = 14$ GeV/c up to 18% (36%) at $p_{\mathrm{T}} = 20$ GeV/c in the 60–80% (0–10%) centrality class.

The contribution of muons from J/ψ decays is estimated by extrapolating the J/ψ p_{T} and y spectra measured by ALICE at forward rapidity ($2.5 < y < 4$) in the interval of $p_{\mathrm{T}} < 12$ GeV/c [49] to a larger kinematic range. Then, the decay muon distributions are estimated with a fast detector simulation using the extrapolated J/ψ distributions as inputs, similar to pp collisions [36]. In the 10% most central collisions, the relative contribution to the inclusive muon distribution varies between 0.5 and 4%, with the maximum fraction at intermediate p_{T} ($4 < p_{\mathrm{T}} < 6$ GeV/c).

The systematic uncertainties of the R_{AA} of muons from heavy-flavour hadron decays at $\sqrt{s_{\mathrm{NN}}} = 5.02$ TeV are evaluated considering the following sources: uncertainties of the inclusive muon yields and background contributions in Pb–Pb collisions, the pp reference, and the normalisation in both pp and Pb–Pb collisions.

The procedure to determine the systematic uncertainty on the inclusive muon yields is similar to that described in [36] and includes the following contributions: i) the muon tracking efficiency (1.5%), ii) the muon trigger efficiency resulting from the intrinsic efficiency of the muon trigger chambers and the response of the trigger algorithm (1.4% (3%) for the MSL (MSH) data sample). A systematic uncertainty of 0.5% is introduced to account for the difference observed with different χ^2 selections for the definition of the matching of tracks reconstructed in the tracking system with those in the trigger system. These systematic uncertainties are approximately independent of centrality and p_{T} in the region of interest. The systematic uncertainty arising from the dependence of $A \times \varepsilon$ on the detector occupancy increases up to 0.5% when going from peripheral to central collisions. Finally, the systematic uncertainty due to the tracking chamber resolution and alignment is based on a Monte Carlo simulation modeling the tracker response with a parameterisation of the tracking chamber resolution and misalignment effects as described in [36, 50]. This systematic uncertainty is negligible for $p_{\mathrm{T}} < 7$ GeV/c and increases up to 12% in the interval $18 < p_{\mathrm{T}} < 20$ GeV/c.

The estimation of the yields of muons from primary $\pi^{\pm}$ and $\mathrm{K}^{\pm}$ decays is subject to systematic uncertainties arising from i) the measured midrapidity spectra of $\pi^{\pm}$ ($\mathrm{K}^{\pm}$) and their p_{T} extrapolation, which increase from about 4% (6%) to 18% (25%), ii) the rapidity extrapolation which results in a systematic uncertainty of about 8.5% (6%) for muons from $\pi^{\pm}$ ($\mathrm{K}^{\pm}$) decays obtained by comparing the results with PYTHIA 6 and PHOJET generators, iii) the rapidity dependence of the p_{T} extrapolation with a systematic uncertainty, obtained from the PYTHIA 8 generator with different CR options, increasing up to about 4% (2%) at $p_{\mathrm{T}} = 20$ GeV/c for $\pi^{\pm}$ ($\mathrm{K}^{\pm}$), and iv) the effect of the absorber which leads to a systematic uncertainty of 4% independently of the muon origin. Combining the four sources, the systematic uncertainty ranges from about 9% (10%) to 21% (27%) as a function of the p_{T} of muons from primary $\pi^{\pm}$ ($\mathrm{K}^{\pm}$) decays. Finally, there is a contribution related to the assumption on the rapidity dependence of the suppression of $\pi^{\pm}$ and $\mathrm{K}^{\pm}$. Based on ATLAS measurements in Pb–Pb collisions at $\sqrt{s_{\mathrm{NN}}} = 2.76$ TeV, which indicate no significant η dependence of the charged-particle R_{AA} up to $|\eta| < 2$ [51], the suppression of $\pi^{\pm}$ and $\mathrm{K}^{\pm}$ is considered to be independent of rapidity up to $y = 4$, and the R_{AA} of $\pi^{\pm}$ and $\mathrm{K}^{\pm}$ is varied conservatively within $\pm 50\%$. This uncertainty is propagated to the decay muons and the difference between the upper and lower limits is further divided by $\sqrt{12}$, corresponding to the RMS of a uniform distribution. This gives a systematic uncertainty on the R_{AA} of heavy-flavour hadron decay muons ranging from about 4.8% ($p_{\mathrm{T}} = 3$ GeV/c) to 1.3% ($p_{\mathrm{T}} = 20$ GeV/c) in the 0–10% centrality class. Furthermore, the effect of the transport code is conservatively evaluated by varying the estimated yield of muons from secondary $\pi^{\pm}$ and $\mathrm{K}^{\pm}$ decays by $\pm 100\%$ and dividing also the difference between lower and upper limits by $\sqrt{12}$. A maximum systematic uncertainty of 0.8% (1.4%) at $p_{\mathrm{T}} = 3$ GeV/c in the 0–10% (60–80%) centrality class is then derived after propagation to the R_{AA} measurement.

The systematic uncertainty of the extracted muon yields from W and $\mathrm{Z}/\gamma^{\star}$ decays is obtained considering the CT10 PDF uncertainty [48] and a different nuclear modification of the PDF (EKS98 [52, 53] was used as well). It amounts to 5.9% (13.2%) for muons from W ($\mathrm{Z}/\gamma^{\star}$) decays.

The systematic uncertainty of the estimated yields of muons from J/ψ decays reflects the uncertainty of the measured J/ψ spectra at forward rapidity and their extrapolation to a wider kinematic region. It varies from about 9% at $p_{\mathrm{T}} = 2$ GeV/c to 34% at $p_{\mathrm{T}} = 20$ GeV/c in central collisions.

Two sources contribute to the systematic uncertainty on the normalisation, the systematic uncertainty of $\langle T_{\mathrm{AA}} \rangle$ values varying from 0.7% (0–10% centrality class) to 2.5% (60–80% centrality class) [20] and the systematic uncertainty of the normalisation factor needed to calculate the number of equivalent MB events in the muon samples of 0.3% (MSL-triggered events) and 0.7% (MSH-triggered events). The latter is evaluated by comparing two different methods (see section 2 and [36]).

The sources of systematic uncertainty affecting the measurement of the pp reference production cross section were evaluated in [36]. The total systematic uncertainty ranges from 2.1% to 15.1%, depending on p_{T}. A global normalisation uncertainty of 2.1% [36] is considered as well. When computing the nuclear modification factor, the systematic uncertainty on track resolution and misalignment is considered to be partially correlated between the pp and Pb–Pb measurements because the pp data were collected just before the Pb–Pb run at $\sqrt{s_{\mathrm{NN}}} = 5.02$ TeV and the detector conditions remained unchanged. The other sources of systematic uncertainties are treated as uncorrelated. The systematic uncertainty on the p_{T}-differential production cross section in pp collisions without including the correlated part of the uncertainty varies from 2.1% to 4.2%. The uncorrelated part of the uncertainty on track resolution and misalignment is due to the different shapes of the p_{T} distribution between pp and Pb–Pb collisions. It is estimated by comparing the results with and without correcting the residual misalignment between data and Monte Carlo when calculating the R_{AA}, as detailed in [36]. The resulting systematic uncertainty assigned to the R_{AA} reaches a maximum of 4.1% at $p_{\mathrm{T}} = 20$ GeV/c.

The various systematic uncertainties are propagated to the measurement of the yields or nuclear modification factors of muons from heavy-flavour hadron decays and added in quadrature, except for the systematic uncertainties on normalisation which are shown separately.

Table 1 reports a summary of the relative systematic uncertainties assigned to the p_{T}-differential yields of muons from heavy-flavour hadron decays in Pb–Pb collisions. The systematic uncertainty on the pp reference, needed for the computation of the R_{AA}, is also reported.

For a direct comparison with lower energy measurements in the same p_{T} interval, the Pb–Pb data sample at $\sqrt{s_{\mathrm{NN}}} = 2.76$ TeV, collected in 2011, was analysed in order to significantly extend the p_{T} interval of the published R_{AA} measurements of muons from heavy-flavour hadron decays, which was limited to $4 < p_{\mathrm{T}} < 10$ GeV/c [32]. Such an improvement is possible due to the larger integrated luminosity (4 $\mu\mathrm{b}^{-1}$ and 71 $\mu\mathrm{b}^{-1}$ for MSL- and MSH-triggered collisions compared to 2.7 $\mu\mathrm{b}^{-1}$) and the use of a high-p_{T} muon-trigger threshold.

The strategy to extract the yields of muons from heavy-flavour hadron decays in Pb–Pb collisions at $\sqrt{s_{\mathrm{NN}}} = 2.76$ TeV is similar to that just discussed for $\sqrt{s_{\mathrm{NN}}} = 5.02$ TeV. Compared to the latter case, the $A \times \varepsilon$ exhibits the same trend as a function of p_{T}, although the values are smaller due to the status of the tracking chambers (larger number of inactive channels). The factor $A \times \varepsilon$ saturates at a value close to 80% in the high-p_{T} region for peripheral collisions (60–80% centrality class). The dependence of the efficiency on the detector occupancy, hence on the collision centrality, is investigated using the embedding procedure as at $\sqrt{s_{\mathrm{NN}}} = 5.02$ TeV. A decrease of the efficiency of 4% from peripheral collisions to the 10% most central collisions is seen. The contributions to the inclusive muon yields from the various background sources at $\sqrt{s_{\mathrm{NN}}} = 2.76$ TeV are compatible with the ones measured at $\sqrt{s_{\mathrm{NN}}} = 5.02$ TeV. The contribution of muons from primary $\pi^{\pm}$ and $\mathrm{K}^{\pm}$ decays with respect to inclusive muons varies between about 3% and 14% in the 0–10% centrality class, the largest values being obtained at $p_{\mathrm{T}} = 3$ GeV/c. On the other hand, the fraction of muons from secondary $\pi^{\pm}$ and $\mathrm{K}^{\pm}$ decays reaches about 1% at $p_{\mathrm{T}} = 3$ GeV/c. The fraction of muons from electroweak-boson decays is significant at high p_{T}, where it reaches about 30% in the interval $16.5 < p_{\mathrm{T}} < 20$ GeV/c for central collisions. Finally, the component of muons from J/ψ decays is small over the whole p_{T} interval with a maximum of 4% at intermediate p_{T} (~ 6 GeV/c) in central collisions. The procedure followed to estimate the systematic uncertainties of the various sources is the same as that described for $\sqrt{s_{\mathrm{NN}}} = 5.02$ TeV, except for the systematic uncertainty of the tracking chamber resolution and alignment which varies linearly with p_{T} as $1\% \times p_{\mathrm{T}}$ (p_{T} in GeV/c) [32]. The p_{T}-differential cross section of muons from heavy-flavour hadron decays in pp collisions at $\sqrt{s} = 2.76$ TeV measured in the intervals $2.5 < y < 4$ and $3 < p_{\mathrm{T}} < 10$ GeV/c

Table 1: Summary of the relative systematic uncertainties of the p_{T}-differential yields of muons from heavy-flavour hadron decays at forward rapidity ($2.5 < y < 4$) in Pb–Pb collisions at $\sqrt{s_{\mathrm{NN}}} = 5.02$ TeV (second and third columns) and 2.76 TeV (fourth column). The systematic uncertainties of the pp reference are also summarised. For the p_{T}-dependent uncertainties, the minimum and maximum values are reported and correspond to the lowest and highest p_{T} interval with the exception of the background of muons from light-hadron decays and the $R_{\mathrm{AA}}^{\pi^{\pm}(\mathrm{K}^{\pm})}(y)$ assumption, where this is the opposite. See the text for details.

Source	$\sqrt{s_{\mathrm{NN}}} = 5.02$ TeV		$\sqrt{s_{\mathrm{NN}}} = 2.76$ TeV
	0–10% centrality class	60–80% centrality class	0–10% centrality class
Tracking efficiency	1.5%	1.5%	2.5%
Trigger efficiency	1.4% (MSL), 3% (MSH)	1.4% (MSL), 3% (MSH)	1.4% (MSL), 2.3% (MSH)
Matching efficiency	0.5%	0.5%	0.5%
$A \times \varepsilon$	0.5%	0	1%
Resolution and alignment	0–12% (0–4.1% on R_{AA})	0–12% (0–4.1% on R_{AA})	$1\% \times p_{\mathrm{T}}$ (p_{T} in GeV/c)
Background subtraction $\mu \leftarrow \pi$	0–1.6%	0–2.5%	0–1.8%
Background subtraction $\mu \leftarrow \mathrm{K}$	0–1.6%	0–2.5%	0–4%
$R_{\mathrm{AA}}^{\pi^{\pm}(\mathrm{K}^{\pm})}(y)$ assumption	1.3–4.8%	1.5–7.8%	1.8–5.2%
Background subtraction $\mu \leftarrow \mathrm{sec.}\pi/\mathrm{K}$	0–0.8%	0–1.4%	0–0.9%
Background subtraction $\mu \leftarrow \mathrm{W}/\mathrm{Z}/\gamma^{\star}$	0–1.6%	0–0.7%	0–3.1%
Background subtraction $\mu \leftarrow \mathrm{J}/\psi$	$< 0.4\%$	$< 0.4\%$	$< 0.3\%$
Normalisation factor	0.3% (MSL), 0.7% (MSH)	0.3% (MSL), 0.7% (MSH)	0.4% (MSL), 1.6% (MSH)
$\langle T_{\mathrm{AA}} \rangle$	0.7%	2.5%	0.9%
pp reference for R_{AA}	2.1–4.2%	2.1–4.2%	15–18% ($3 < p_{\mathrm{T}} < 10$ GeV/c data) 30–34% ($10 < p_{\mathrm{T}} < 20$ GeV/c extrapolation)
pp reference (global) for R_{AA}	2.1%	2.1%	1.9%

is used for the R_{AA} computation [32]. The measured production cross section is extrapolated up to $p_T = 20$ GeV/c using fixed-order plus next-to-leading logarithms (FONLL) calculations [54, 55]. The systematic uncertainty of the p_T-differential production cross section in pp collisions at $\sqrt{s} = 2.76$ TeV varies within 15–18%, depending on p_T in $3 < p_T < 10$ GeV/c. At higher p_T, the systematic uncertainty, which includes the systematic uncertainty on the measurement and FONLL calculations, reaches 30–34%.

A summary of all systematic uncertainties taken into account in the measurement of the p_T-differential yields of muons from heavy-flavour hadron decays at $\sqrt{s_{NN}} = 2.76$ TeV is reported in Table 1, including the uncertainties of the pp reference.

4 Results and model comparisons

The p_T-differential yields of muons from heavy-flavour hadron decays normalised to the equivalent number of MB events at forward rapidity ($2.5 < y < 4$) in central (0–10%), semi-central (20–40%), and peripheral (60–80%) Pb–Pb collisions at $\sqrt{s_{NN}} = 5.02$ TeV are shown in Fig. 1 (upper panel). The same observable measured in central (0–10%) Pb–Pb collisions at $\sqrt{s_{NN}} = 2.76$ TeV is displayed in the lower panel of Fig. 1. The measurements are performed over a wide p_T range from 3 to 20 GeV/c for all centrality classes.

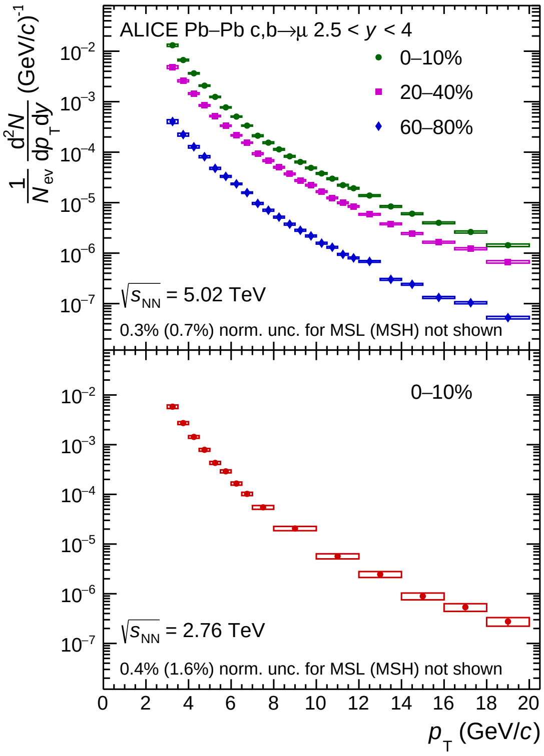

Figure 1: The p_T-differential yields of muons from heavy-flavour hadron decays at forward rapidity ($2.5 < y < 4$) in central (0–10%), semi-central (20–40%), and peripheral (60–80%) Pb–Pb collisions at $\sqrt{s_{NN}} = 5.02$ TeV (upper panel), and in central (0–10%) Pb–Pb collisions at $\sqrt{s_{NN}} = 2.76$ TeV (lower panel). Statistical uncertainties (vertical bars) and systematic uncertainties (open boxes) are shown. The additional systematic uncertainty on normalisation in Pb–Pb collisions at $\sqrt{s_{NN}} = 5.02$ (2.76) TeV for MSL- and MSH-triggered events, respectively, is not shown (see Table 1).

The p_T-differential R_{AA} of muons from heavy-flavour hadron decays at forward rapidity ($2.5 < y < 4$) in Pb–Pb collisions at $\sqrt{s_{NN}} = 5.02$ TeV is presented in Fig. 2 for central (0–10%), semi-central (20–40%),

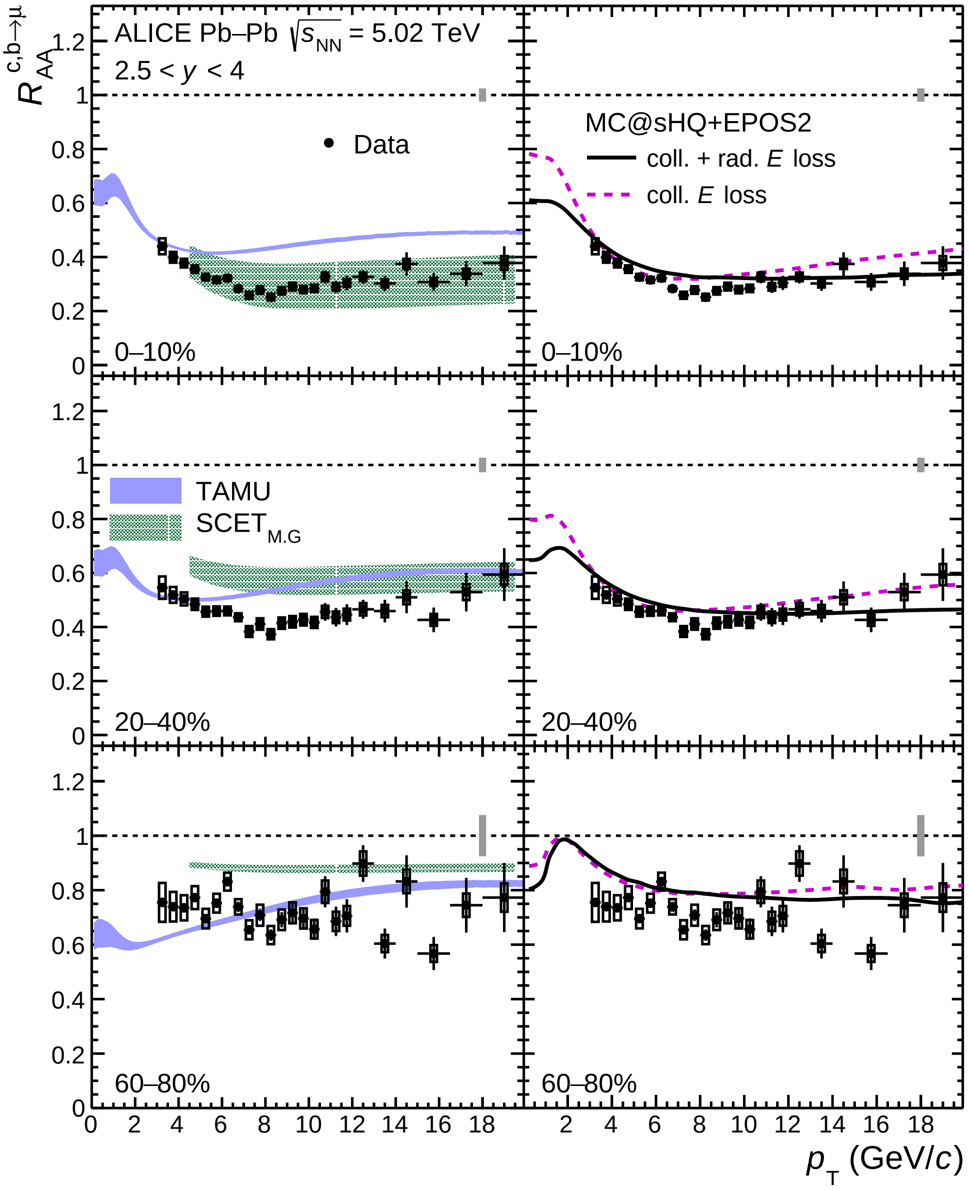

Figure 2: The p_T-differential nuclear modification factor of muons from heavy-flavour hadron decays at forward rapidity ($2.5 < y < 4$) in central (0–10%, top), semi-central (20–40%, middle), and peripheral (60–80%, bottom) Pb–Pb collisions at $\sqrt{s_{NN}} = 5.02$ TeV (symbols). Statistical (vertical bars) and systematic uncertainties (open boxes) are shown. The filled boxes centered at $R_{AA} = 1$ represent the normalisation uncertainty. Horizontal bars reflect the bin widths. Left: the measured R_{AA} is compared with the TAMU and SCET models [56, 57] displayed with their uncertainty bands. Right: the measured R_{AA} is compared with MC@sHQ+EPOS2 model calculations with pure collisional energy loss (full lines) and a combination of collisional and radiative energy loss (dashed lines) [58, 59]. See the text for details.

and peripheral (60–80%) collisions. The vertical bars are the statistical uncertainties and the empty boxes are the systematic uncertainties. The horizontal bars correspond to the width of the p_T interval and the values are shown at the centre of the bin. The uncertainty of the normalisation including the uncertainty of $\langle T_{AA} \rangle$ and the muon trigger normalisations in Pb–Pb collisions, and of the integrated luminosity in pp collisions is shown as full boxes at $R_{AA} = 1$. An increasing reduction of the yield of muons from heavy-flavour hadron decays with increasing centrality with respect to the pp reference scaled by the average nuclear overlap function is clearly seen. The suppression is largest at intermediate p_T, in the interval

$6 < p_{\mathrm{T}} < 8$ GeV/c and reaches a factor of about three in the 10% most central collisions. The suppression becomes smaller with decreasing p_{T} and presents no significant p_{T} dependence for $p_{\mathrm{T}} > 10$ GeV/c. In minimum bias p–Pb collisions at $\sqrt{s_{\mathrm{NN}}} = 5.02$ TeV, where the formation of an extended QGP is not expected, the nuclear modification factor R_{pPb} of muons from heavy-flavour hadron decays is consistent with unity at $p_{\mathrm{T}} > 6$ GeV/c [60]. The latter measurement confirms that the strong suppression observed in Pb–Pb collisions results from final-state interactions of charm and beauty quarks with the QGP. The evolution of R_{AA} as a function of centrality is compatible with the dependence of the heavy-quark energy loss on the medium density and the average path length in the medium, which both are larger in central than in peripheral collisions.

The measured R_{AA} is compared with various model predictions such as TAMU [56] and SCET [57] (Fig. 2, left), and MC@sHQ+EPOS2 [58, 59] (Fig. 2, right). In the TAMU model, the interactions are described by elastic collisions only. The SCET model implements medium-induced gluon radiation via modified splitting functions with finite quark masses. These SCET calculations depend on the coupling constant g which describes the coupling strength between hard partons and the QGP medium. Its value is $g = 1.9$–2. In the MC@sHQ+EPOS2 model, two different options are considered, including either energy loss from medium-induced gluon radiation and collisional (elastic) processes or only collisional energy loss. In the scenario with pure collisional energy loss, the scattering rates are scaled by a global factor K larger than unity ($K = 1.5$) in order to reproduce the R_{AA} and elliptic flow of open heavy-flavour hadrons measured at midrapidity at the LHC [58]. With a combination of collisional and radiative energy loss, the scaling factor is $K = 0.8$. All these models also consider a nuclear modification of the PDF (EPS09) [17]. Note that in the MC@sHQ+EPOS2 model shadowing is not considered for beauty-quark production. In addition to independent fragmentation, a contribution of hadronisation via quark recombination is included in all models with the exception of SCET. The SCET calculations provide a fair description of the data in central collisions but deviate from the data in peripheral collisions. The TAMU calculations underestimate the suppression at $p_{\mathrm{T}} > 6$ GeV/c in central and semi-central collisions, in particular. Both versions of the MC@sHQ+EPOS2 model, without and with radiative energy loss, describe the measurement within uncertainties for all centrality classes over the entire p_{T} interval.

The results obtained at forward rapidity for muons from heavy-flavour hadron decays at $\sqrt{s_{\mathrm{NN}}} = 5.02$ TeV complement those obtained at midrapidity for the electrons from heavy-flavour hadron decays [24] by the ALICE collaboration as well as the prompt D-meson [25, 26] and beauty measurements via $\mathrm{B}^{\pm}$ mesons [31], non-prompt D^0 [31] and J/ψ [30] by the ALICE and CMS collaborations. The measured R_{AA} of muons from heavy-flavour hadron decays for $p_{\mathrm{T}} > 8$ GeV/c is compatible with that obtained for beauty (D^0 and J/ψ from beauty hadrons, $\mathrm{B}^{\pm}$) for $p_{\mathrm{T}}^{\mathrm{hadron}} > 10$ GeV/c [30, 31] within uncertainties, although in a different kinematic region (different p_{T} and y intervals).

A comparison of the R_{AA} of muons from heavy-flavour hadron decays in the 10% most central Pb–Pb collisions at $\sqrt{s_{\mathrm{NN}}} = 2.76$ and 5.02 TeV is presented in Fig. 3. The comparison illustrates the improvement of the precision of the measurement at $\sqrt{s_{\mathrm{NN}}} = 5.02$ TeV with respect to that at $\sqrt{s_{\mathrm{NN}}} = 2.76$ TeV. The total systematic uncertainty on the R_{AA} at $\sqrt{s_{\mathrm{NN}}} = 5.02$ TeV is reduced by a factor of about 3 to 6, depending on p_{T}, compared to the same measurement at $\sqrt{s_{\mathrm{NN}}} = 2.76$ TeV using the 2011 data sample. The reasons for such an improvement are twofold. The detector conditions were more stable during the $\sqrt{s_{\mathrm{NN}}} = 5.02$ TeV than the $\sqrt{s_{\mathrm{NN}}} = 2.76$ TeV data taking campaign and therefore better described in the simulations. Moreover, as the pp data at $\sqrt{s} = 5.02$ TeV were collected just a few days before the Pb–Pb run at $\sqrt{s_{\mathrm{NN}}} = 5.02$ TeV, the detector conditions were comparable and the systematic uncertainty on alignment and resolution between the two systems partially cancel when computing R_{AA}, as discussed in section 3. The precision of the present measurement at $\sqrt{s_{\mathrm{NN}}} = 2.76$ TeV increased by a factor 1.1–1.6 compared to the published results at the same centre-of-mass energy [32], mainly due to a better understanding of the detector response and a new data-driven strategy for the estimation of the contribution of muons from primary light-hadron decays. The comparison between the results obtained

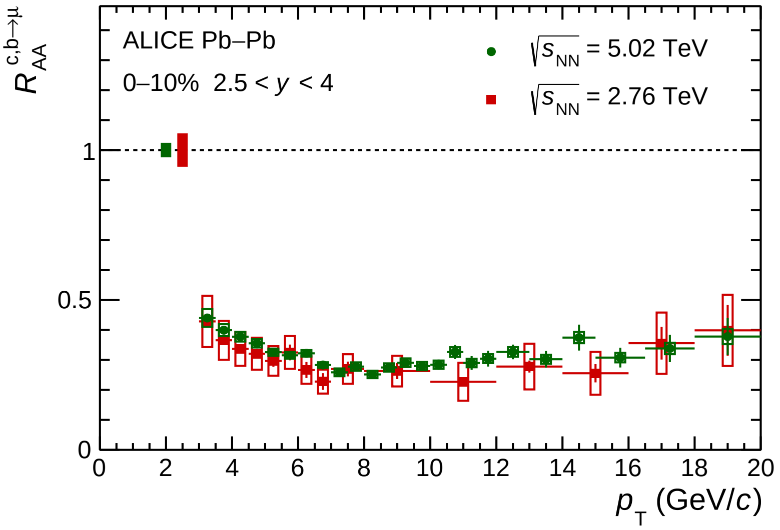

Figure 3: Comparison of the $p_{\rm T}$-differential nuclear modification factor of muons from heavy-flavour hadron decays at forward rapidity ($2.5 < y < 4$) in central Pb–Pb collisions at $\sqrt{s_{\rm NN}} = 5.02$ TeV (green symbols) and $\sqrt{s_{\rm NN}} = 2.76$ TeV (red symbols). Statistical (vertical bars) and systematic uncertainties (open boxes) are shown. The filled boxes centered at $R_{\rm AA} = 1$ are the normalisation uncertainties. Horizontal bars represent the bin widths.

at the two centre-of-mass energies indicates that the suppression of heavy quarks at $\sqrt{s_{\rm NN}} = 5.02$ TeV is similar to that at $\sqrt{s_{\rm NN}} = 2.76$ TeV, as already observed in the midrapidity region for electrons from heavy-flavour hadron decays [22, 24] and prompt D mesons [25]. This similarity between the $R_{\rm AA}$ measurements at the two energies may result from the interplay of the following two effects as discussed in [61]: a flattening of the $p_{\rm T}$ spectra of charm and beauty quarks with increasing collision energy, and a medium temperature estimated to be higher by about 7% at $\sqrt{s_{\rm NN}} = 5.02$ TeV than at 2.76 TeV. The former would decrease the heavy-quark suppression (increase the $R_{\rm AA}$) by about 5% if the medium temperature remains unchanged, while the latter would increase the suppression (decrease the $R_{\rm AA}$) by about 10% (5%) for charm (beauty) quarks.

The measured $R_{\rm AA}$ at $\sqrt{s_{\rm NN}} = 2.76$ TeV is consistent with that measured for muons from heavy-flavour hadron decays in $|\eta| < 1$ with the ATLAS detector [21] and for electrons from heavy-flavour hadron decays in the interval $\langle y \rangle < 0.6$ by the ALICE collaboration [28]. The $R_{\rm AA}$ of muons from heavy-flavour hadron decays at $\sqrt{s_{\rm NN}} = 5.02$ TeV is also compatible with that measured at midrapidity for electrons from heavy-flavour hadron decays [24]. This confirms that heavy quarks suffer a strong in-medium energy loss over a wide rapidity interval.

The $p_{\rm T}$ distributions of muons from heavy-flavour hadron decays are sensitive to energy loss of both charm and beauty quarks. Due to the decay kinematics and the charm- and beauty-quark $p_{\rm T}$-differential production cross sections, one expects that for $p_{\rm T} \lesssim 5$ GeV/c the distributions are predominantly sensitive to the charm in-medium energy loss. FONLL calculations [54, 55] predict that in pp collisions at $\sqrt{s} = 5.02$ TeV more than 70% of muons from heavy-flavour hadron decays originate from beauty quarks in the high-$p_{\rm T}$ region ($p_{\rm T} > 10$ GeV/c) and this contribution reaches 75% in the interval $18 < p_{\rm T} < 20$ GeV/c. Therefore, the strong suppression of muons from heavy-flavour hadron decays in the high-$p_{\rm T}$ region is expected to be dominated by the in-medium energy loss of beauty quarks. In order to further interpret the results, Fig. 4 shows a comparison with MC@sHQ+EPOS2 predictions for muons from charm- and beauty-hadron decays, separately, and for muons from the combination of the two, in central (0–10%) Pb–Pb collisions at $\sqrt{s_{\rm NN}} = 5.02$ TeV (top) and 2.76 TeV (bottom). The predictions considering the combination of elastic and radiative energy loss and pure elastic energy loss are shown in the left and right panels, respectively. Both versions of the MC@sHQ+EPOS2 model provide a fair

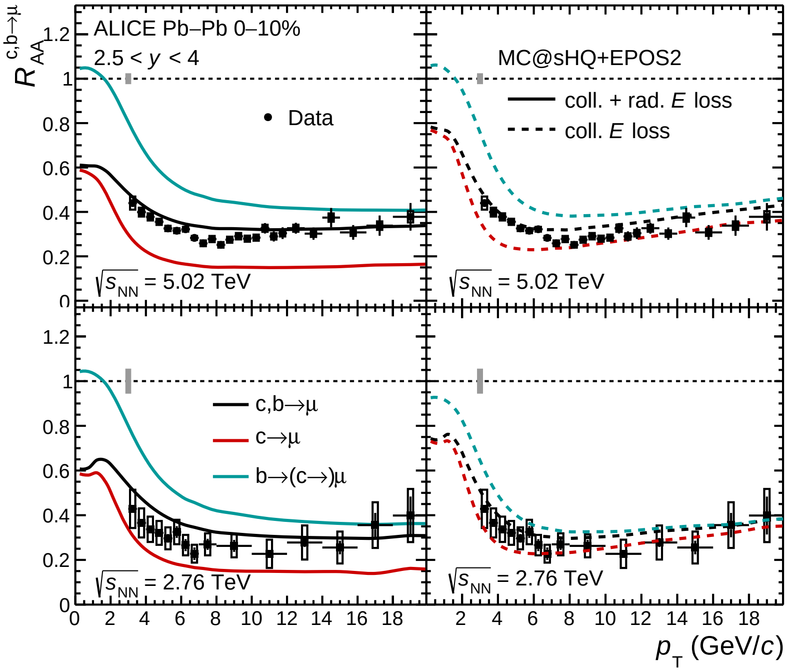

Figure 4: Comparison of the p_T-differential nuclear modification factors of muons from heavy-flavour hadron decays at forward rapidity ($2.5 < y < 4$) in central Pb–Pb collisions at $\sqrt{s_{NN}} = 5.02$ TeV (top) and $\sqrt{s_{NN}} = 2.76$ TeV (bottom) with MC@sHQ+EPOS2 calculations with different scenarios considering either a combination of collisional and radiative energy loss (left) or a pure collisional energy loss (right). The predictions are shown for muons from charm- and beauty-hadron decays, muons from charm-hadron decays and muons from beauty-hadron decays.

description of the measured R_{AA} of muons from heavy-flavour hadron decays in central Pb–Pb collisions at $\sqrt{s_{NN}} = 5.02$ TeV within uncertainties. A similar agreement between data and MC@sHQ+EPOS2 is achieved at $\sqrt{s_{NN}} = 2.76$ TeV although the model tends to slightly overestimate the measured R_{AA} at low/intermediate p_T. The measured R_{AA} at large p_T is closer to the model calculations for muons from beauty-hadron decays than for muons from charm-hadron decays when considering both elastic and radiative energy loss. For the scenario involving only collisional energy loss, the predicted difference between the suppression of muons from charm and beauty-hadron decays is less pronounced. The predicted ratio of the p_T-differential R_{AA} of muons from beauty-hadron decays to that of muons from charm-hadron decays for $p_T > 10$ GeV/c is in the range 1.2–1.4 for the scenario involving only collisional energy loss and in the range 2.5–2.8 when considering both elastic and radiative energy loss, depending on p_T and centre-of-mass energy. It is worth mentioning that the MC@sHQ+EPOS2 model is characterised by a large running coupling constant α_s and a reduced Debye mass in the elastic heavy-quark scattering generating the radiation [62]. As a consequence, the radiative energy loss neglects finite path-length effects due to the gluon formation outside the QGP and is overestimated at high p_T. Such an effect is expected to be more pronounced for charm quarks than for beauty quarks due to the dead-cone effect [8].

5 Conclusions

In summary, the p_T-differential nuclear modification factor, R_{AA}, of muons from semi-leptonic decays of charm and beauty hadrons was measured at forward rapidity ($2.5 < y < 4$) for the first time over the wide p_T interval $3 < p_T < 20$ GeV/c in central, semi-central, and peripheral Pb–Pb collisions at $\sqrt{s_{NN}} = 5.02$ TeV, and in central Pb–Pb collisions at $\sqrt{s_{NN}} = 2.76$ TeV with reduced systematic uncertainties compared to previous measurements.

The measured R_{AA} shows a clear evidence of a strong suppression, up to a factor of three in the 10% most central collisions with respect to the binary-scaled pp reference, for both collision energies. This suppression pattern is compatible with a large heavy-quark in-medium energy loss. The strong suppression which persists in the high-p_{T} region, up to $p_{\mathrm{T}} = 20$ GeV/c, indicates that beauty quarks lose a significant fraction of their energy in the medium. The suppression becomes weaker from central to peripheral collisions. The R_{AA} evolution with the collision centrality reflects the dependence of energy loss on the path length in the QGP and the QGP energy density. These new precise R_{AA} measurements at forward rapidity in Pb–Pb collisions at $\sqrt{s_{\mathrm{NN}}} = 5.02$ TeV with smaller uncertainties with respect to same measurements at $\sqrt{s_{\mathrm{NN}}} = 2.76$ TeV, currently only accessible by ALICE in central collisions, have the potential to discriminate between different model calculations and in-medium parton energy loss scenarios. The R_{AA} in central collisions is in fair agreement with model calculations considering both collisional and radiative energy loss. The MC@sHQ+EPOS2 transport model including a hydrodynamic description of the medium, coupled with different implementations of the in-medium parton energy loss, describes the measured R_{AA} well over the whole p_{T} interval in central, semi-central, and peripheral collisions within uncertainties. This study brings new important constraints on the relative in-medium energy loss of charm and beauty quarks.

Acknowledgements

The ALICE Collaboration would like to thank all its engineers and technicians for their invaluable contributions to the construction of the experiment and the CERN accelerator teams for the outstanding performance of the LHC complex. The ALICE Collaboration gratefully acknowledges the resources and support provided by all Grid centres and the Worldwide LHC Computing Grid (WLCG) collaboration. The ALICE Collaboration acknowledges the following funding agencies for their support in building and running the ALICE detector: A. I. Alikhanyan National Science Laboratory (Yerevan Physics Institute) Foundation (ANSL), State Committee of Science and World Federation of Scientists (WFS), Armenia; Austrian Academy of Sciences, Austrian Science Fund (FWF): [M 2467-N36] and Nationalstiftung für Forschung, Technologie und Entwicklung, Austria; Ministry of Communications and High Technologies, National Nuclear Research Center, Azerbaijan; Conselho Nacional de Desenvolvimento Científico e Tecnológico (CNPq), Financiadora de Estudos e Projetos (Finep), Fundação de Amparo à Pesquisa do Estado de São Paulo (FAPESP) and Universidade Federal do Rio Grande do Sul (UFRGS), Brazil; Ministry of Education of China (MOEC) , Ministry of Science & Technology of China (MSTC) and National Natural Science Foundation of China (NSFC), China; Ministry of Science and Education and Croatian Science Foundation, Croatia; Centro de Aplicaciones Tecnológicas y Desarrollo Nuclear (CEADEN), Cubaenergía, Cuba; Ministry of Education, Youth and Sports of the Czech Republic, Czech Republic; The Danish Council for Independent Research | Natural Sciences, the VILLUM FONDEN and Danish National Research Foundation (DNRF), Denmark; Helsinki Institute of Physics (HIP), Finland; Commissariat à l'Energie Atomique (CEA) and Institut National de Physique Nucléaire et de Physique des Particules (IN2P3) and Centre National de la Recherche Scientifique (CNRS), France; Bundesministerium für Bildung und Forschung (BMBF) and GSI Helmholtzzentrum für Schwerionenforschung GmbH, Germany; General Secretariat for Research and Technology, Ministry of Education, Research and Religions, Greece; National Research, Development and Innovation Office, Hungary; Department of Atomic Energy Government of India (DAE), Department of Science and Technology, Government of India (DST), University Grants Commission, Government of India (UGC) and Council of Scientific and Industrial Research (CSIR), India; Indonesian Institute of Science, Indonesia; Istituto Nazionale di Fisica Nucleare (INFN), Italy; Institute for Innovative Science and Technology , Nagasaki Institute of Applied Science (IIST), Japanese Ministry of Education, Culture, Sports, Science and Technology (MEXT) and Japan Society for the Promotion of Science (JSPS) KAKENHI, Japan; Consejo Nacional de Ciencia (CONACYT) y Tecnología, through Fondo de Cooperación Internacional en Ciencia y Tecnología (FONCICYT) and Dirección General de Asuntos del Personal Academico (DGAPA), Mexico;

Nederlandse Organisatie voor Wetenschappelijk Onderzoek (NWO), Netherlands; The Research Council of Norway, Norway; Commission on Science and Technology for Sustainable Development in the South (COMSATS), Pakistan; Pontificia Universidad Católica del Perú, Peru; Ministry of Science and Higher Education, National Science Centre and WUT ID-UB, Poland; Korea Institute of Science and Technology Information and National Research Foundation of Korea (NRF), Republic of Korea; Ministry of Education and Scientific Research, Institute of Atomic Physics and Ministry of Research and Innovation and Institute of Atomic Physics, Romania; Joint Institute for Nuclear Research (JINR), Ministry of Education and Science of the Russian Federation, National Research Centre Kurchatov Institute, Russian Science Foundation and Russian Foundation for Basic Research, Russia; Ministry of Education, Science, Research and Sport of the Slovak Republic, Slovakia; National Research Foundation of South Africa, South Africa; Swedish Research Council (VR) and Knut & Alice Wallenberg Foundation (KAW), Sweden; European Organization for Nuclear Research, Switzerland; Suranaree University of Technology (SUT), National Science and Technology Development Agency (NSDTA) and Office of the Higher Education Commission under NRU project of Thailand, Thailand; Turkish Atomic Energy Agency (TAEK), Turkey; National Academy of Sciences of Ukraine, Ukraine; Science and Technology Facilities Council (STFC), United Kingdom; National Science Foundation of the United States of America (NSF) and United States Department of Energy, Office of Nuclear Physics (DOE NP), United States of America.

References

[1] **Wuppertal-Budapest** Collaboration, S. Borsanyi, Z. Fodor, C. Hoelbling, S. D. Katz, S. Krieg, C. Ratti, and K. K. Szabo, “Is there still any T_c mystery in lattice QCD? Results with physical masses in the continuum limit III”, *JHEP* **09** (2010) 073, `arXiv:1005.3508 [hep-lat]`.

[2] A. Bazavov *et al.*, “The chiral and deconfinement aspects of the QCD transition”, *Phys. Rev.* **D85** (2012) 054503, `arXiv:1111.1710 [hep-lat]`.

[3] S. Borsanyi, Z. Fodor, C. Hoelbling, S. D. Katz, S. Krieg, and K. K. Szabo, “Full result for the QCD equation of state with 2+1 flavors”, *Phys. Lett. B* **730** (2014) 99–104, `arXiv:1309.5258 [hep-lat]`.

[4] **HotQCD** Collaboration, A. Bazavov *et al.*, “Chiral crossover in QCD at zero and non-zero chemical potentials”, *Phys. Lett. B* **795** (2019) 15–21, `arXiv:1812.08235 [hep-lat]`.

[5] A. Andronic *et al.*, “Heavy-flavour and quarkonium production in the LHC era: from proton-proton to heavy-ion collisions”, *Eur. Phys. J.* **C76** no. 3, (2016) 107, `arXiv:1506.03981 [nucl-ex]`.

[6] F.-M. Liu and S.-X. Liu, “Quark-gluon plasma formation time and direct photons from heavy ion collisions”, *Phys. Rev.* **C89** no. 3, (2014) 034906, `arXiv:1212.6587 [nucl-th]`.

[7] R. Baier, Y. L. Dokshitzer, A. H. Mueller, S. Peigne, and D. Schiff, “Radiative energy loss and p_{T} broadening of high-energy partons in nuclei”, *Nucl. Phys.* **B484** (1997) 265–282, `arXiv:hep-ph/9608322 [hep-ph]`.

[8] Y. L. Dokshitzer and D. E. Kharzeev, “Heavy quark colorimetry of QCD matter”, *Phys. Lett.* **B519** (2001) 199–206, `arXiv:hep-ph/0106202 [hep-ph]`.

[9] M. Djordjevic and M. Gyulassy, “Heavy quark radiative energy loss in QCD matter”, *Nucl. Phys.* **A733** (2004) 265–298, `arXiv:nucl-th/0310076 [nucl-th]`.

[10] B.-W. Zhang, E. Wang, and X.-N. Wang, “Heavy quark energy loss in nuclear medium”, *Phys. Rev. Lett.* **93** (2004) 072301, `arXiv:nucl-th/0309040`.

[11] S. Wicks, W. Horowitz, M. Djordjevic, and M. Gyulassy, "Heavy quark jet quenching with collisional plus radiative energy loss and path length fluctuations", *Nucl. Phys.* **A783** (2007) 493–496, `arXiv:nucl-th/0701063 [nucl-th]`.

[12] P. B. Gossiaux, J. Aichelin, T. Gousset, and V. Guiho, "Competition of Heavy Quark Radiative and Collisional Energy Loss in Deconfined Matter", *J. Phys.* **G37** (2010) 094019, `arXiv:1001.4166 [hep-ph]`.

[13] N. Armesto, C. A. Salgado, and U. A. Wiedemann, "Medium induced gluon radiation off massive quarks fills the dead cone", *Phys. Rev.* **D69** (2004) 114003, `arXiv:hep-ph/0312106 [hep-ph]`.

[14] H. van Hees, V. Greco, and R. Rapp, "Heavy-quark probes of the quark-gluon plasma at RHIC", *Phys. Rev.* **C73** (2006) 034913, `arXiv:nucl-th/0508055 [nucl-th]`.

[15] V. Greco, C. M. Ko, and R. Rapp, "Quark coalescence for charmed mesons in ultrarelativistic heavy ion collisions", *Phys. Lett.* **B595** (2004) 202–208, `arXiv:nucl-th/0312100 [nucl-th]`.

[16] A. Andronic, P. Braun-Munzinger, K. Redlich, and J. Stachel, "Statistical hadronization of charm in heavy ion collisions at SPS, RHIC and LHC", *Phys. Lett.* **B571** (2003) 36–44, `arXiv:nucl-th/0303036 [nucl-th]`.

[17] K. J. Eskola, H. Paukkunen, and C. A. Salgado, "EPS09: A New Generation of NLO and LO Nuclear Parton Distribution Functions", *JHEP* **04** (2009) 065, `arXiv:0902.4154 [hep-ph]`.

[18] B. Z. Kopeliovich, J. Nemchik, A. Schafer, and A. V. Tarasov, "Cronin effect in hadron production off nuclei", *Phys. Rev. Lett.* **88** (2002) 232303, `arXiv:hep-ph/0201010 [hep-ph]`.

[19] I. Vitev, "Non-Abelian energy loss in cold nuclear matter", *Phys. Rev.* **C75** (2007) 064906, `arXiv:hep-ph/0703002 [hep-ph]`.

[20] **ALICE** Collaboration, "Centrality determination in heavy ion collisions." ALICE-PUBLIC-2018-011, 2018. `http://cds.cern.ch/record/2636623`.

[21] **ATLAS** Collaboration, M. Aaboud *et al.*, "Measurement of the suppression and azimuthal anisotropy of muons from heavy-flavor decays in Pb+Pb collisions at $\sqrt{s_{\rm NN}} = 2.76$ TeV with the ATLAS detector", *Phys. Rev.* **C98** no. 4, (2018) 044905, `arXiv:1805.05220 [nucl-ex]`.

[22] **ALICE** Collaboration, S. Acharya *et al.*, "Measurements of low-$p_{\rm T}$ electrons from semileptonic heavy-flavour hadron decays at mid-rapidity in pp and Pb–Pb collisions at $\sqrt{s_{\rm NN}} = 2.76$ TeV", *JHEP* **10** (2018) 061, `arXiv:1805.04379 [nucl-ex]`.

[23] **STAR** Collaboration, J. Adam *et al.*, "Centrality and transverse momentum dependence of $\rm D^0$-meson production at mid-rapidity in Au+Au collisions at $\sqrt{s_{\rm NN}} = 200\,$GeV", *Phys. Rev.* **C99** no. 3, (2019) 034908, `arXiv:1812.10224 [nucl-ex]`.

[24] **ALICE** Collaboration, S. Acharya *et al.*, "Measurement of electrons from semileptonic heavy-flavour hadron decays at midrapidity in pp and Pb–Pb collisions at $\sqrt{s_{\rm NN}}$ = 5.02 TeV", *Phys. Lett.* **B804** (2020) 135377, `arXiv:1910.09110 [nucl-ex]`.

[25] **ALICE** Collaboration, S. Acharya *et al.*, "Measurement of $\rm D^0$, $\rm D^+$, $\rm D^{*+}$ and $\rm D_s^+$ production in Pb–Pb collisions at $\sqrt{s_{\rm NN}} = 5.02$ TeV", *JHEP* **10** (2018) 174, `arXiv:1804.09083 [nucl-ex]`.

[26] **CMS** Collaboration, A. M. Sirunyan *et al.*, "Nuclear modification factor of $\rm D^0$ mesons in Pb–Pb collisions at $\sqrt{s_{\rm NN}} = 5.02$ TeV", *Phys. Lett.* **B782** (2018) 474–496, `arXiv:1708.04962 [nucl-ex]`.

[27] **ALICE** Collaboration, J. Adam *et al.*, "Transverse momentum dependence of D-meson production in Pb–Pb collisions at $\sqrt{s_{\mathrm{NN}}} = 2.76$ TeV", *JHEP* **03** (2016) 081, `arXiv:1509.06888 [nucl-ex]`.

[28] **ALICE** Collaboration, J. Adam *et al.*, "Measurement of the production of high-p_{T} electrons from heavy-flavour hadron decays in Pb–Pb collisions at $\sqrt{s_{\mathrm{NN}}}$ = 2.76 TeV", *Phys. Lett.* **B771** (2017) 467–481, `arXiv:1609.07104 [nucl-ex]`.

[29] **CMS** Collaboration, A. M. Sirunyan *et al.*, "Measurement of the $\mathrm{B}^{\pm}$ Meson Nuclear Modification Factor in Pb–Pb Collisions at $\sqrt{s_{\mathrm{NN}}} = 5.02$ TeV", *Phys. Rev. Lett.* **119** no. 15, (2017) 152301, `arXiv:1705.04727 [hep-ex]`.

[30] **CMS** Collaboration, A. M. Sirunyan *et al.*, "Measurement of prompt and nonprompt charmonium suppression in Pb–Pb collisions at 5.02 TeV", *Eur. Phys. J.* **C78** no. 6, (2018) 509, `arXiv:1712.08959 [nucl-ex]`.

[31] **CMS** Collaboration, A. M. Sirunyan *et al.*, "Studies of Beauty Suppression via Nonprompt D^0 Mesons in Pb–Pb Collisions at $Q^2 = 4$ GeV^2", *Phys. Rev. Lett.* **123** no. 2, (2019) 022001, `arXiv:1810.11102 [hep-ex]`.

[32] **ALICE** Collaboration, B. Abelev *et al.*, "Production of muons from heavy flavour decays at forward rapidity in pp and Pb–Pb collisions at $\sqrt{s_{NN}}$ = 2.76 TeV", *Phys. Rev. Lett.* **109** (2012) 112301, `arXiv:1205.6443 [hep-ex]`.

[33] **ALICE** Collaboration, K. Aamodt *et al.*, "The ALICE experiment at the CERN LHC", *JINST* **3** (2008) S08002.

[34] **ALICE** Collaboration, B. B. Abelev *et al.*, "Performance of the ALICE Experiment at the CERN LHC", *Int. J. Mod. Phys.* **A29** (2014) 1430044, `arXiv:1402.4476 [nucl-ex]`.

[35] **ALICE** Collaboration, J. Adam *et al.*, "Centrality dependence of the charged-particle multiplicity density at midrapidity in Pb–Pb collisions at $\sqrt{s_{\mathrm{NN}}}$ = 5.02 TeV", *Phys. Rev. Lett.* **116** no. 22, (2016) 222302, `arXiv:1512.06104 [nucl-ex]`.

[36] **ALICE** Collaboration, S. Acharya *et al.*, "Production of muons from heavy-flavour hadron decays in pp collisions at $\sqrt{s}$ = 5.02 TeV", *JHEP* **09** (2019) 008, `arXiv:1905.07207 [nucl-ex]`.

[37] **ALICE** Collaboration, S. Acharya *et al.*, "Production of charged pions, kaons and (anti-)protons in Pb-Pb and inelastic pp collisions at $\sqrt{s_{\mathrm{NN}}}$ = 5.02 TeV", *Phys. Rev. C* **101** no. 4, (2020) 044907, `arXiv:1910.07678 [nucl-ex]`.

[38] T. Sjostrand, S. Mrenna, and P. Z. Skands, "PYTHIA 6.4 Physics and Manual", *JHEP* **05** (2006) 026, `arXiv:hep-ph/0603175 [hep-ph]`.

[39] R. Engel, J. Ranft, and S. Roesler, "Hard diffraction in hadron-hadron interactions and in photoproduction", *Phys. Rev.* **D52** (Aug, 1995) 1459–1468.

[40] T. Sjöstrand, S. Ask, J. R. Christiansen, R. Corke, N. Desai, P. Ilten, S. Mrenna, S. Prestel, C. O. Rasmussen, and P. Z. Skands, "An Introduction to PYTHIA 8.2", *Comput. Phys. Commun.* **191** (2015) 159–177, `arXiv:1410.3012 [hep-ph]`.

[41] X.-N. Wang and M. Gyulassy, "HIJING: A Monte Carlo model for multiple jet production in pp, pA and AA collisions", *Phys. Rev.* **D44** (1991) 3501–3516.

[42] R. Brun, F. Bruyant, F. Carminati, S. Giani, M. Maire, A. McPherson, G. Patrick, and L. Urban, "GEANT Detector Description and Simulation Tool." CERN-W5013, CERN-W-5013, W5013, W-5013, 1994.

[43] S. Alioli, P. Nason, C. Oleari, and E. Re, "NLO vector-boson production matched with shower in POWHEG", *JHEP* **07** (2008) 060, `arXiv:0805.4802 [hep-ph]`.

[44] **CMS** Collaboration, S. Chatrchyan *et al.*, "Study of Z boson production in Pb–Pb collisions at $\sqrt{s_{\rm NN}}$ = 2.76 TeV", *Phys. Rev. Lett.* **106** (2011) 212301, `arXiv:1102.5435 [nucl-ex]`.

[45] **CMS** Collaboration, S. Chatrchyan *et al.*, "Study of Z production in PbPb and pp collisions at $\sqrt{s_{\rm NN}} = 2.76$ TeV in the dimuon and dielectron decay channels", *JHEP* **03** (2015) 022, `arXiv:1410.4825 [nucl-ex]`.

[46] **ATLAS** Collaboration, G. Aad *et al.*, "Measurement of the production and lepton charge asymmetry of W bosons in Pb+Pb collisions at $\sqrt{\mathbf{s_{NN}}} = 2.76\ TeV$ with the ATLAS detector", *Eur. Phys. J. C* **75** no. 1, (2015) 23, `arXiv:1408.4674 [hep-ex]`.

[47] **CMS** Collaboration, V. Khachatryan *et al.*, "Study of Z boson production in p–Pb collisions at $\sqrt{s_{\rm NN}} = 5.02$ TeV", *Phys. Lett. B* **759** (2016) 36–57, `arXiv:1512.06461 [hep-ex]`.

[48] H.-L. Lai, M. Guzzi, J. Huston, Z. Li, P. M. Nadolsky, J. Pumplin, and C. P. Yuan, "New parton distributions for collider physics", *Phys. Rev.* **D82** (2010) 074024, `arXiv:1007.2241 [hep-ph]`.

[49] **ALICE** Collaboration, J. Adam *et al.*, "J/ψ suppression at forward rapidity in Pb–Pb collisions at $\sqrt{s_{\rm NN}} = 5.02$ TeV", *Phys. Lett.* **B766** (2017) 212–224, `arXiv:1606.08197 [nucl-ex]`.

[50] **ALICE** Collaboration, J. Adam *et al.*, "W and Z boson production in p–Pb collisions at $\sqrt{s_{\rm NN}}$ = 5.02 TeV", *JHEP* **02** (2017) 077, `arXiv:1611.03002 [nucl-ex]`.

[51] **ATLAS** Collaboration, G. Aad *et al.*, "Measurement of charged-particle spectra in Pb+Pb collisions at $\sqrt{s_{\rm NN}} = 2.76$ TeV with the ATLAS detector at the LHC", *JHEP* **09** (2015) 050, `arXiv:1504.04337 [hep-ex]`.

[52] K. J. Eskola, H. Honkanen, V. J. Kolhinen, and C. A. Salgado, "Global DGLAP fit analyses of the npdf: EKS98 and HKM", `arXiv:hep-ph/0302170 [hep-ph]`.

[53] **Heavy Quarks and Quarkonia Working Group, Jet Physics Working Group, PDFs, Shadowing and p+A Working Group, Photons Working Group** Collaboration, M. L. Mangano, H. Satz, and U. A. Wiedemann, *Hard Probes in Heavy Ion Collisions at the LHC: [report of the 4 working groups].* CERN Yellow Reports: Monographs. CERN, Geneva, 2004. `https://cds.cern.ch/record/815037`. Report of the 4 working groups completed by Oct 2003, following 3 plenary meetings held from Oct 2001 - Oct 2002 of the CERN Theory Workshop on Hard Probes in Heavy Ion Collisions at the LHC.

[54] M. Cacciari, M. Greco, and P. Nason, "The $p_{\rm T}$ spectrum in heavy flavor hadroproduction", *JHEP* **05** (1998) 007, `arXiv:hep-ph/9803400 [hep-ph]`.

[55] M. Cacciari, S. Frixione, N. Houdeau, M. L. Mangano, P. Nason, and G. Ridolfi, "Theoretical predictions for charm and bottom production at the LHC", *JHEP* **10** (2012) 137, `arXiv:1205.6344 [hep-ph]`.

[56] M. He, R. J. Fries, and R. Rapp, "Heavy Flavor at the Large Hadron Collider in a Strong Coupling Approach", *Phys. Lett.* **B735** (2014) 445–450, `arXiv:1401.3817 [nucl-th]`.

[57] Z.-B. Kang, F. Ringer, and I. Vitev, “Effective field theory approach to open heavy flavor production in heavy-ion collisions”, *JHEP* **03** (2017) 146, `arXiv:1610.02043 [hep-ph]`.

[58] M. Nahrgang, J. Aichelin, P. B. Gossiaux, and K. Werner, “Influence of hadronic bound states above T_c on heavy-quark observables in Pb+Pb collisions at the CERN Large Hadron Collider”, *Phys. Rev.* **C89** no. 1, (2014) 014905, `arXiv:1305.6544 [hep-ph]`.

[59] M. Nahrgang, J. Aichelin, P. B. Gossiaux, and K. Werner, “Azimuthal correlations of heavy quarks in Pb + Pb collisions at $\sqrt{s} = 2.76$ TeV at the CERN Large Hadron Collider”, *Phys. Rev.* **C90** no. 2, (2014) 024907, `arXiv:1305.3823 [hep-ph]`.

[60] **ALICE** Collaboration, S. Acharya *et al.*, “Production of muons from heavy-flavour hadron decays in p-Pb collisions at $\sqrt{s_{\mathbf{NN}}} = \mathbf{5.02}$ TeV”, *Phys. Lett.* **B770** (2017) 459–472, `arXiv:1702.01479 [nucl-ex]`.

[61] M. Djordjevic and M. Djordjevic, “Predictions of heavy-flavor suppression at 5.1 TeV Pb+Pb collisions at the CERN Large Hadron Collider”, *Phys. Rev.* **C92** no. 2, (2015) 024918, `arXiv:1505.04316 [nucl-th]`.

[62] A. Beraudo *et al.*, “Extraction of Heavy-Flavor Transport Coefficients in QCD Matter”, *Nucl. Phys.* **A979** (2018) 21–86, `arXiv:1803.03824 [nucl-th]`.

A The ALICE Collaboration

ALICE Collaboration

S. Acharya[142], D. Adamová[96], A. Adler[74], J. Adolfsson[81], G. Aglieri Rinella[34], M. Agnello[30], N. Agrawal[54,9], Z. Ahammed[142], S. Ahmad[16], S.U. Ahn[76], Z. Akbar[51], A. Akindinov[93], M. Al-Turany[108], D.S.D. Albuquerque[123], D. Aleksandrov[89], B. Alessandro[59], H.M. Alfanda[6], R. Alfaro Molina[71], B. Ali[16], Y. Ali[14], A. Alici[26,9,54], N. Alizadehvandchali[126], A. Alkin[34], J. Alme[21], T. Alt[68], L. Altenkamper[21], I. Altsybeev[114], M.N. Anaam[6], C. Andrei[48], D. Andreou[91], A. Andronic[145], M. Angeletti[34], V. Anguelov[105], T. Antičić[109], F. Antinori[57], P. Antonioli[54], N. Apadula[80], L. Aphecetche[116], H. Appelshäuser[68], S. Arcelli[26], R. Arnaldi[59], M. Arratia[80], I.C. Arsene[20], M. Arslandok[147,105], A. Augustinus[34], R. Averbeck[108], S. Aziz[78], M.D. Azmi[16], A. Badalà[56], Y.W. Baek[41], X. Bai[108], R. Bailhache[68], R. Bala[102], A. Balbino[30], A. Baldisseri[138], M. Ball[43], D. Banerjee[3], R. Barbera[27], L. Barioglio[25], M. Barlou[85], G.G. Barnaföldi[146], L.S. Barnby[95], V. Barret[135], C. Bartels[128], K. Barth[34], E. Bartsch[68], F. Baruffaldi[28], N. Bastid[135], S. Basu[81,144], G. Batigne[116], B. Batyunya[75], D. Bauri[49], J.L. Bazo Alba[113], I.G. Bearden[90], C. Beattie[147], I. Belikov[137], A.D.C. Bell Hechavarria[145], F. Bellini[34], R. Bellwied[126], S. Belokurova[114], V. Belyaev[94], G. Bencedi[69,146], S. Beole[25], A. Bercuci[48], Y. Berdnikov[99], A. Berdnikova[105], D. Berenyi[146], D. Berzano[59], M.G. Besoiu[67], L. Betev[34], P.P. Bhaduri[142], A. Bhasin[102], I.R. Bhat[102], M.A. Bhat[3], B. Bhattacharjee[42], P. Bhattacharya[23], A. Bianchi[25], L. Bianchi[25], N. Bianchi[52], J. Bielčík[37], J. Bielčíková[96], A. Bilandzic[106], G. Biro[146], S. Biswas[3], J.T. Blair[120], D. Blau[89], M.B. Blidaru[108], C. Blume[68], G. Boca[140], F. Bock[97], A. Bogdanov[94], S. Boi[23], J. Bok[61], L. Boldizsár[146], A. Bolozdynya[94], M. Bombara[38], G. Bonomi[141], H. Borel[138], A. Borissov[82,94], H. Bossi[147], E. Botta[25], L. Bratrud[68], P. Braun-Munzinger[108], M. Bregant[122], M. Broz[37], G.E. Bruno[107,33], M.D. Buckland[128], D. Budnikov[110], H. Buesching[68], S. Bufalino[30], O. Bugnon[116], P. Buhler[115], P. Buncic[34], Z. Buthelezi[72,132], J.B. Butt[14], S.A. Bysiak[119], D. Caffarri[91], A. Caliva[108], E. Calvo Villar[113], J.M.M. Camacho[121], R.S. Camacho[45], P. Camerini[24], A.A. Capon[115], F. Carnesecchi[26], R. Caron[138], J. Castillo Castellanos[138], A.J. Castro[131], E.A.R. Casula[55], F. Catalano[30], C. Ceballos Sanchez[75], P. Chakraborty[49], S. Chandra[142], W. Chang[6], S. Chapeland[34], M. Chartier[128], S. Chattopadhyay[142], S. Chattopadhyay[111], A. Chauvin[23], C. Cheshkov[136], B. Cheynis[136], V. Chibante Barroso[34], D.D. Chinellato[123], S. Cho[61], P. Chochula[34], P. Christakoglou[91], C.H. Christensen[90], P. Christiansen[81], T. Chujo[134], C. Cicalo[55], L. Cifarelli[26,9], F. Cindolo[54], M.R. Ciupek[108], G. Clai[II,54], J. Cleymans[125], F. Colamaria[53], J.S. Colburn[112], D. Colella[53], A. Collu[80], M. Colocci[34,26], M. Concas[III,59], G. Conesa Balbastre[79], Z. Conesa del Valle[78], G. Contin[24,60], J.G. Contreras[37], T.M. Cormier[97], P. Cortese[31], M.R. Cosentino[124], F. Costa[34], S. Costanza[140], P. Crochet[135], E. Cuautle[69], P. Cui[6], L. Cunqueiro[97], T. Dahms[106], A. Dainese[57], F.P.A. Damas[116,138], M.C. Danisch[105], A. Danu[67], D. Das[111], I. Das[111], P. Das[87], P. Das[3], S. Das[3], S. Dash[49], S. De[87], A. De Caro[29], G. de Cataldo[53], L. De Cilladi[25], J. de Cuveland[39], A. De Falco[23], D. De Gruttola[29,9], N. De Marco[59], C. De Martin[24], S. De Pasquale[29], S. Deb[50], H.F. Degenhardt[122], K.R. Deja[143], S. Delsanto[25], W. Deng[6], P. Dhankher[19,49], D. Di Bari[33], A. Di Mauro[34], R.A. Diaz[7], T. Dietel[125], P. Dillenseger[68], Y. Ding[6], R. Divià[34], D.U. Dixit[19], Ø. Djuvsland[21], U. Dmitrieva[63], J. Do[61], A. Dobrin[67], B. Dönigus[68], O. Dordic[20], A.K. Dubey[142], A. Dubla[108,91], S. Dudi[101], M. Dukhishyam[87], P. Dupieux[135], T.M. Eder[145], R.J. Ehlers[97], V.N. Eikeland[21], D. Elia[53], B. Erazmus[116], F. Erhardt[100], A. Erokhin[114], M.R. Ersdal[21], B. Espagnon[78], G. Eulisse[34], D. Evans[112], S. Evdokimov[92], L. Fabbietti[106], M. Faggin[28], J. Faivre[79], F. Fan[6], A. Fantoni[52], M. Fasel[97], P. Fecchio[30], A. Feliciello[59], G. Feofilov[114], A. Fernández Téllez[45], A. Ferrero[138], A. Ferretti[25], A. Festanti[34], V.J.G. Feuillard[105], J. Figiel[119], S. Filchagin[110], D. Finogeev[63], F.M. Fionda[21], G. Fiorenza[53], F. Flor[126], A.N. Flores[120], S. Foertsch[72], P. Foka[108], S. Fokin[89], E. Fragiacomo[60], U. Fuchs[34], C. Furget[79], A. Furs[63], M. Fusco Girard[29], J.J. Gaardhøje[90], M. Gagliardi[25], A.M. Gago[113], A. Gal[137], C.D. Galvan[121], P. Ganoti[85], C. Garabatos[108], J.R.A. Garcia[45], E. Garcia-Solis[10], K. Garg[116], C. Gargiulo[34], A. Garibli[88], K. Garner[145], P. Gasik[106],

E.F. Gauger[120], M.B. Gay Ducati[70], M. Germain[116], J. Ghosh[111], P. Ghosh[142], S.K. Ghosh[3], M. Giacalone[26], P. Gianotti[52], P. Giubellino[108,59], P. Giubilato[28], A.M.C. Glaenzer[138], P. Glässel[105], V. Gonzalez[144], L.H. González-Trueba[71], S. Gorbunov[39], L. Görlich[119], S. Gotovac[35], V. Grabski[71], L.K. Graczykowski[143], K.L. Graham[112], L. Greiner[80], A. Grelli[62], C. Grigoras[34], V. Grigoriev[94], A. Grigoryan[I,1], S. Grigoryan[75], O.S. Groettvik[21], F. Grosa[59], J.F. Grosse-Oetringhaus[34], R. Grosso[108], R. Guernane[79], M. Guilbaud[116], M. Guittiere[116], K. Gulbrandsen[90], T. Gunji[133], A. Gupta[102], R. Gupta[102], I.B. Guzman[45], R. Haake[147], M.K. Habib[108], C. Hadjidakis[78], H. Hamagaki[83], G. Hamar[146], M. Hamid[6], R. Hannigan[120], M.R. Haque[143,87], A. Harlenderova[108], J.W. Harris[147], A. Harton[10], J.A. Hasenbichler[34], H. Hassan[97], D. Hatzifotiadou[54,9], P. Hauer[43], L.B. Havener[147], S. Hayashi[133], S.T. Heckel[106], E. Hellbär[68], H. Helstrup[36], T. Herman[37], E.G. Hernandez[45], G. Herrera Corral[8], F. Herrmann[145], K.F. Hetland[36], H. Hillemanns[34], C. Hills[128], B. Hippolyte[137], B. Hohlweger[106], J. Honermann[145], G.H. Hong[148], D. Horak[37], A. Hornung[68], S. Hornung[108], R. Hosokawa[15], P. Hristov[34], C. Huang[78], C. Hughes[131], P. Huhn[68], T.J. Humanic[98], H. Hushnud[111], L.A. Husova[145], N. Hussain[42], D. Hutter[39], J.P. Iddon[34,128], R. Ilkaev[110], H. Ilyas[14], M. Inaba[134], G.M. Innocenti[34], M. Ippolitov[89], A. Isakov[37,96], M.S. Islam[111], M. Ivanov[108], V. Ivanov[99], V. Izucheev[92], B. Jacak[80], N. Jacazio[34,54], P.M. Jacobs[80], S. Jadlovska[118], J. Jadlovsky[118], S. Jaelani[62], C. Jahnke[122], M.J. Jakubowska[143], M.A. Janik[143], T. Janson[74], M. Jercic[100], O. Jevons[112], M. Jin[126], F. Jonas[97,145], P.G. Jones[112], J. Jung[68], M. Jung[68], A. Jusko[112], P. Kalinak[64], A. Kalweit[34], V. Kaplin[94], S. Kar[6], A. Karasu Uysal[77], D. Karatovic[100], O. Karavichev[63], T. Karavicheva[63], P. Karczmarczyk[143], E. Karpechev[63], A. Kazantsev[89], U. Kebschull[74], R. Keidel[47], M. Keil[34], B. Ketzer[43], Z. Khabanova[91], A.M. Khan[6], S. Khan[16], A. Khanzadeev[99], Y. Kharlov[92], A. Khatun[16], A. Khuntia[119], B. Kileng[36], B. Kim[61], B. Kim[134], D. Kim[148], D.J. Kim[127], E.J. Kim[73], H. Kim[17], J. Kim[148], J.S. Kim[41], J. Kim[105], J. Kim[148], J. Kim[73], M. Kim[105], S. Kim[18], T. Kim[148], T. Kim[148], S. Kirsch[68], I. Kisel[39], S. Kiselev[93], A. Kisiel[143], J.L. Klay[5], C. Klein[68], J. Klein[34,59], S. Klein[80], C. Klein-Bösing[145], M. Kleiner[68], T. Klemenz[106], A. Kluge[34], A.G. Knospe[126], C. Kobdaj[117], M.K. Köhler[105], T. Kollegger[108], A. Kondratyev[75], N. Kondratyeva[94], E. Kondratyuk[92], J. Konig[68], S.A. Konigstorfer[106], P.J. Konopka[34], G. Kornakov[143], L. Koska[118], O. Kovalenko[86], V. Kovalenko[114], M. Kowalski[119], I. Králik[64], A. Kravčáková[38], L. Kreis[108], M. Krivda[112,64], F. Krizek[96], K. Krizkova Gajdosova[37], M. Kroesen[105], M. Krüger[68], E. Kryshen[99], M. Krzewicki[39], V. Kučera[34], C. Kuhn[137], P.G. Kuijer[91], L. Kumar[101], S. Kundu[87], P. Kurashvili[86], A. Kurepin[63], A.B. Kurepin[63], A. Kuryakin[110], S. Kushpil[96], J. Kvapil[112], M.J. Kweon[61], J.Y. Kwon[61], Y. Kwon[148], S.L. La Pointe[39], P. La Rocca[27], Y.S. Lai[80], A. Lakrathok[117], M. Lamanna[34], R. Langoy[130], K. Lapidus[34], A. Lardeux[20], P. Larionov[52], E. Laudi[34], L. Lautner[34], R. Lavicka[37], T. Lazareva[114], R. Lea[24], J. Lee[134], S. Lee[148], J. Lehrbach[39], R.C. Lemmon[95], I. León Monzón[121], E.D. Lesser[19], M. Lettrich[34], P. Lévai[146], X. Li[11], X.L. Li[6], J. Lien[130], R. Lietava[112], B. Lim[17], S.H. Lim[17], V. Lindenstruth[39], A. Lindner[48], C. Lippmann[108], A. Liu[19], J. Liu[128], I.M. Lofnes[21], V. Loginov[94], C. Loizides[97], P. Loncar[35], J.A. Lopez[105], X. Lopez[135], E. López Torres[7], J.R. Luhder[145], M. Lunardon[28], G. Luparello[60], Y.G. Ma[40], A. Maevskaya[63], M. Mager[34], S.M. Mahmood[20], T. Mahmoud[43], A. Maire[137], R.D. Majka[I,147], M. Malaev[99], Q.W. Malik[20], L. Malinina[IV,75], D. Mal'Kevich[93], N. Mallick[50], P. Malzacher[108], G. Mandaglio[32,56], V. Manko[89], F. Manso[135], V. Manzari[53], Y. Mao[6], M. Marchisone[136], J. Mareš[66], G.V. Margagliotti[24], A. Margotti[54], A. Marín[108], C. Markert[120], M. Marquard[68], N.A. Martin[105], P. Martinengo[34], J.L. Martinez[126], M.I. Martínez[45], G. Martínez García[116], S. Masciocchi[108], M. Masera[25], A. Masoni[55], L. Massacrier[78], A. Mastroserio[139,53], A.M. Mathis[106], O. Matonoha[81], P.F.T. Matuoka[122], A. Matyja[119], C. Mayer[119], F. Mazzaschi[25], M. Mazzilli[53], M.A. Mazzoni[58], A.F. Mechler[68], F. Meddi[22], Y. Melikyan[63], A. Menchaca-Rocha[71], C. Mengke[6], E. Meninno[115,29], A.S. Menon[126], M. Meres[13], S. Mhlanga[125], Y. Miake[134], L. Micheletti[25], L.C. Migliorin[136], D.L. Mihaylov[106], K. Mikhaylov[75,93], A.N. Mishra[146,69], D. Miśkowiec[108], A. Modak[3], N. Mohammadi[34], A.P. Mohanty[62], B. Mohanty[87], M. Mohisin Khan[V,16], Z. Moravcova[90], C. Mordasini[106], D.A. Moreira De Godoy[145], L.A.P. Moreno[45], I. Morozov[63], A. Morsch[34], T. Mrnjavac[34], V. Muccifora[52], E. Mudnic[35], D. Mühlheim[145], S. Muhuri[142], J.D. Mulligan[80], A. Mulliri[23,55], M.G. Munhoz[122], R.H. Munzer[68], H. Murakami[133],

S. Murray[125], L. Musa[34], J. Musinsky[64], C.J. Myers[126], J.W. Myrcha[143], B. Naik[49], R. Nair[86], B.K. Nandi[49], R. Nania[54,9], E. Nappi[53], M.U. Naru[14], A.F. Nassirpour[81], C. Nattrass[131], R. Nayak[49], S. Nazarenko[110], A. Neagu[20], L. Nellen[69], S.V. Nesbo[36], G. Neskovic[39], D. Nesterov[114], B.S. Nielsen[90], S. Nikolaev[89], S. Nikulin[89], V. Nikulin[99], F. Noferini[54,9], S. Noh[12], P. Nomokonov[75], J. Norman[128,79], N. Novitzky[134], P. Nowakowski[143], A. Nyanin[89], J. Nystrand[21], M. Ogino[83], A. Ohlson[81], J. Oleniacz[143], A.C. Oliveira Da Silva[131], M.H. Oliver[147], B.S. Onnerstad[127], C. Oppedisano[59], A. Ortiz Velasquez[69], T. Osako[46], A. Oskarsson[81], J. Otwinowski[119], K. Oyama[83], Y. Pachmayer[105], V. Pacik[90], S. Padhan[49], D. Pagano[141], G. Paić[69], J. Pan[144], S. Panebianco[138], P. Pareek[142], J. Park[61], J.E. Parkkila[127], S. Parmar[101], S.P. Pathak[126], B. Paul[23], J. Pazzini[141], H. Pei[6], T. Peitzmann[62], X. Peng[6], L.G. Pereira[70], H. Pereira Da Costa[138], D. Peresunko[89], G.M. Perez[7], S. Perrin[138], Y. Pestov[4], V. Petráček[37], M. Petrovici[48], R.P. Pezzi[70], S. Piano[60], M. Pikna[13], P. Pillot[116], O. Pinazza[54,34], L. Pinsky[126], C. Pinto[27], S. Pisano[9,52], M. Płoskoń[80], M. Planinic[100], F. Pliquett[68], M.G. Poghosyan[97], B. Polichtchouk[92], N. Poljak[100], A. Pop[48], S. Porteboeuf-Houssais[135], J. Porter[80], V. Pozdniakov[75], S.K. Prasad[3], R. Preghenella[54], F. Prino[59], C.A. Pruneau[144], I. Pshenichnov[63], M. Puccio[34], S. Qiu[91], L. Quaglia[25], R.E. Quishpe[126], S. Ragoni[112], J. Rak[127], A. Rakotozafindrabe[138], L. Ramello[31], F. Rami[137], S.A.R. Ramirez[45], R. Raniwala[103], S. Raniwala[103], S.S. Räsänen[44], R. Rath[50], I. Ravasenga[91], K.F. Read[97,131], A.R. Redelbach[39], K. Redlich[VI,86], A. Rehman[21], P. Reichelt[68], F. Reidt[34], R. Renfordt[68], Z. Rescakova[38], K. Reygers[105], A. Riabov[99], V. Riabov[99], T. Richert[81,90], M. Richter[20], P. Riedler[34], W. Riegler[34], F. Riggi[27], C. Ristea[67], S.P. Rode[50], M. Rodríguez Cahuantzi[45], K. Røed[20], R. Rogalev[92], E. Rogochaya[75], D. Rohr[34], D. Röhrich[21], P.F. Rojas[45], P.S. Rokita[143], F. Ronchetti[52], A. Rosano[32,56], E.D. Rosas[69], A. Rossi[57], A. Rotondi[140], A. Roy[50], P. Roy[111], O.V. Rueda[81], R. Rui[24], B. Rumyantsev[75], A. Rustamov[88], E. Ryabinkin[89], Y. Ryabov[99], A. Rybicki[119], H. Rytkonen[127], O.A.M. Saarimaki[44], R. Sadek[116], S. Sadovsky[92], J. Saetre[21], K. Šafařík[37], S.K. Saha[142], S. Saha[87], B. Sahoo[49], P. Sahoo[49], R. Sahoo[50], S. Sahoo[65], D. Sahu[50], P.K. Sahu[65], J. Saini[142], S. Sakai[134], S. Sambyal[102], V. Samsonov[99,94], D. Sarkar[144], N. Sarkar[142], P. Sarma[42], V.M. Sarti[106], M.H.P. Sas[147,62], J. Schambach[97,120], H.S. Scheid[68], C. Schiaua[48], R. Schicker[105], A. Schmah[105], C. Schmidt[108], H.R. Schmidt[104], M.O. Schmidt[105], M. Schmidt[104], N.V. Schmidt[97,68], A.R. Schmier[131], J. Schukraft[89], Y. Schutz[137], K. Schwarz[108], K. Schweda[108], G. Scioli[26], E. Scomparin[59], J.E. Seger[15], Y. Sekiguchi[133], D. Sekihata[133], I. Selyuzhenkov[108,94], S. Senyukov[137], J.J. Seo[61], D. Serebryakov[63], L. Šerkšnytė[106], A. Sevcenco[67], A. Shabanov[63], A. Shabetai[116], R. Shahoyan[34], W. Shaikh[111], A. Shangaraev[92], A. Sharma[101], H. Sharma[119], M. Sharma[102], N. Sharma[101], S. Sharma[102], O. Sheibani[126], A.I. Sheikh[142], K. Shigaki[46], M. Shimomura[84], S. Shirinkin[93], Q. Shou[40], Y. Sibiriak[89], S. Siddhanta[55], T. Siemiarczuk[86], D. Silvermyr[81], G. Simatovic[91], G. Simonetti[34], B. Singh[106], R. Singh[87], R. Singh[102], R. Singh[50], V.K. Singh[142], V. Singhal[142], T. Sinha[111], B. Sitar[13], M. Sitta[31], T.B. Skaali[20], M. Slupecki[44], N. Smirnov[147], R.J.M. Snellings[62], C. Soncco[113], J. Song[126], A. Songmoolnak[117], F. Soramel[28], S. Sorensen[131], I. Sputowska[119], J. Stachel[105], I. Stan[67], P.J. Steffanic[131], S.F. Stiefelmaier[105], D. Stocco[116], M.M. Storetvedt[36], L.D. Stritto[29], C.P. Stylianidis[91], A.A.P. Suaide[122], T. Sugitate[46], C. Suire[78], M. Suljic[34], R. Sultanov[93], M. Šumbera[96], V. Sumberia[102], S. Sumowidagdo[51], S. Swain[65], A. Szabo[13], I. Szarka[13], U. Tabassam[14], S.F. Taghavi[106], G. Taillepied[135], J. Takahashi[123], G.J. Tambave[21], S. Tang[135,6], Z. Tang[129], M. Tarhini[116], M.G. Tarzila[48], A. Tauro[34], G. Tejeda Muñoz[45], A. Telesca[34], L. Terlizzi[25], C. Terrevoli[126], S. Thakur[142], D. Thomas[120], F. Thoresen[90], R. Tieulent[136], A. Tikhonov[63], A.R. Timmins[126], M. Tkacik[118], A. Toia[68], N. Topilskaya[63], M. Toppi[52], F. Torales-Acosta[19], S.R. Torres[37,8], A. Trifiró[32,56], S. Tripathy[69], T. Tripathy[49], S. Trogolo[28], G. Trombetta[33], L. Tropp[38], V. Trubnikov[2], W.H. Trzaska[127], T.P. Trzcinski[143], B.A. Trzeciak[62], A. Tumkin[110], R. Turrisi[57], T.S. Tveter[20], K. Ullaland[21], E.N. Umaka[126], A. Uras[136], G.L. Usai[23], M. Vala[38], N. Valle[140], S. Vallero[59], N. van der Kolk[62], L.V.R. van Doremalen[62], M. van Leeuwen[62], P. Vande Vyvre[34], D. Varga[146], Z. Varga[146], M. Varga-Kofarago[146], A. Vargas[45], M. Vasileiou[85], A. Vasiliev[89], O. Vázquez Doce[106], V. Vechernin[114], E. Vercellin[25], S. Vergara Limón[45], L. Vermunt[62], R. Vértesi[146], M. Verweij[62], L. Vickovic[35], Z. Vilakazi[132], O. Villalobos Baillie[112], G. Vino[53],

A. Vinogradov[89], T. Virgili[29], V. Vislavicius[90], A. Vodopyanov[75], B. Volkel[34], M.A. Völkl[104], K. Voloshin[93], S.A. Voloshin[144], G. Volpe[33], B. von Haller[34], I. Vorobyev[106], D. Voscek[118], J. Vrláková[38], B. Wagner[21], M. Weber[115], S.G. Weber[145], A. Wegrzynek[34], S.C. Wenzel[34], J.P. Wessels[145], J. Wiechula[68], J. Wikne[20], G. Wilk[86], J. Wilkinson[108,9], G.A. Willems[145], E. Willsher[112], B. Windelband[105], M. Winn[138], W.E. Witt[131], J.R. Wright[120], Y. Wu[129], R. Xu[6], S. Yalcin[77], Y. Yamaguchi[46], K. Yamakawa[46], S. Yang[21], S. Yano[46,138], Z. Yin[6], H. Yokoyama[62], I.-K. Yoo[17], J.H. Yoon[61], S. Yuan[21], A. Yuncu[105], V. Yurchenko[2], V. Zaccolo[24], A. Zaman[14], C. Zampolli[34], H.J.C. Zanoli[62], N. Zardoshti[34], A. Zarochentsev[114], P. Závada[66], N. Zaviyalov[110], H. Zbroszczyk[143], M. Zhalov[99], S. Zhang[40], X. Zhang[6], Y. Zhang[129], Z. Zhang[6], V. Zherebchevskii[114], Y. Zhi[11], D. Zhou[6], Y. Zhou[90], J. Zhu[6,108], Y. Zhu[6], A. Zichichi[9,26], G. Zinovjev[2], N. Zurlo[141]

Affiliation Notes

[I] Deceased
[II] Also at: Italian National Agency for New Technologies, Energy and Sustainable Economic Development (ENEA), Bologna, Italy
[III] Also at: Dipartimento DET del Politecnico di Torino, Turin, Italy
[IV] Also at: M.V. Lomonosov Moscow State University, D.V. Skobeltsyn Institute of Nuclear, Physics, Moscow, Russia
[V] Also at: Department of Applied Physics, Aligarh Muslim University, Aligarh, India
[VI] Also at: Institute of Theoretical Physics, University of Wroclaw, Poland

Collaboration Institutes

[1] A.I. Alikhanyan National Science Laboratory (Yerevan Physics Institute) Foundation, Yerevan, Armenia
[2] Bogolyubov Institute for Theoretical Physics, National Academy of Sciences of Ukraine, Kiev, Ukraine
[3] Bose Institute, Department of Physics and Centre for Astroparticle Physics and Space Science (CAPSS), Kolkata, India
[4] Budker Institute for Nuclear Physics, Novosibirsk, Russia
[5] California Polytechnic State University, San Luis Obispo, California, United States
[6] Central China Normal University, Wuhan, China
[7] Centro de Aplicaciones Tecnológicas y Desarrollo Nuclear (CEADEN), Havana, Cuba
[8] Centro de Investigación y de Estudios Avanzados (CINVESTAV), Mexico City and Mérida, Mexico
[9] Centro Fermi - Museo Storico della Fisica e Centro Studi e Ricerche “Enrico Fermi’, Rome, Italy
[10] Chicago State University, Chicago, Illinois, United States
[11] China Institute of Atomic Energy, Beijing, China
[12] Chungbuk National University, Cheongju, Republic of Korea
[13] Comenius University Bratislava, Faculty of Mathematics, Physics and Informatics, Bratislava, Slovakia
[14] COMSATS University Islamabad, Islamabad, Pakistan
[15] Creighton University, Omaha, Nebraska, United States
[16] Department of Physics, Aligarh Muslim University, Aligarh, India
[17] Department of Physics, Pusan National University, Pusan, Republic of Korea
[18] Department of Physics, Sejong University, Seoul, Republic of Korea
[19] Department of Physics, University of California, Berkeley, California, United States
[20] Department of Physics, University of Oslo, Oslo, Norway

[21] Department of Physics and Technology, University of Bergen, Bergen, Norway
[22] Dipartimento di Fisica dell'Università 'La Sapienza' and Sezione INFN, Rome, Italy
[23] Dipartimento di Fisica dell'Università and Sezione INFN, Cagliari, Italy
[24] Dipartimento di Fisica dell'Università and Sezione INFN, Trieste, Italy
[25] Dipartimento di Fisica dell'Università and Sezione INFN, Turin, Italy
[26] Dipartimento di Fisica e Astronomia dell'Università and Sezione INFN, Bologna, Italy
[27] Dipartimento di Fisica e Astronomia dell'Università and Sezione INFN, Catania, Italy
[28] Dipartimento di Fisica e Astronomia dell'Università and Sezione INFN, Padova, Italy
[29] Dipartimento di Fisica 'E.R. Caianiello' dell'Università and Gruppo Collegato INFN, Salerno, Italy
[30] Dipartimento DISAT del Politecnico and Sezione INFN, Turin, Italy
[31] Dipartimento di Scienze e Innovazione Tecnologica dell'Università del Piemonte Orientale and INFN Sezione di Torino, Alessandria, Italy
[32] Dipartimento di Scienze MIFT, Università di Messina, Messina, Italy
[33] Dipartimento Interateneo di Fisica 'M. Merlin' and Sezione INFN, Bari, Italy
[34] European Organization for Nuclear Research (CERN), Geneva, Switzerland
[35] Faculty of Electrical Engineering, Mechanical Engineering and Naval Architecture, University of Split, Split, Croatia
[36] Faculty of Engineering and Science, Western Norway University of Applied Sciences, Bergen, Norway
[37] Faculty of Nuclear Sciences and Physical Engineering, Czech Technical University in Prague, Prague, Czech Republic
[38] Faculty of Science, P.J. Šafárik University, Košice, Slovakia
[39] Frankfurt Institute for Advanced Studies, Johann Wolfgang Goethe-Universität Frankfurt, Frankfurt, Germany
[40] Fudan University, Shanghai, China
[41] Gangneung-Wonju National University, Gangneung, Republic of Korea
[42] Gauhati University, Department of Physics, Guwahati, India
[43] Helmholtz-Institut für Strahlen- und Kernphysik, Rheinische Friedrich-Wilhelms-Universität Bonn, Bonn, Germany
[44] Helsinki Institute of Physics (HIP), Helsinki, Finland
[45] High Energy Physics Group, Universidad Autónoma de Puebla, Puebla, Mexico
[46] Hiroshima University, Hiroshima, Japan
[47] Hochschule Worms, Zentrum für Technologietransfer und Telekommunikation (ZTT), Worms, Germany
[48] Horia Hulubei National Institute of Physics and Nuclear Engineering, Bucharest, Romania
[49] Indian Institute of Technology Bombay (IIT), Mumbai, India
[50] Indian Institute of Technology Indore, Indore, India
[51] Indonesian Institute of Sciences, Jakarta, Indonesia
[52] INFN, Laboratori Nazionali di Frascati, Frascati, Italy
[53] INFN, Sezione di Bari, Bari, Italy
[54] INFN, Sezione di Bologna, Bologna, Italy
[55] INFN, Sezione di Cagliari, Cagliari, Italy
[56] INFN, Sezione di Catania, Catania, Italy
[57] INFN, Sezione di Padova, Padova, Italy
[58] INFN, Sezione di Roma, Rome, Italy
[59] INFN, Sezione di Torino, Turin, Italy
[60] INFN, Sezione di Trieste, Trieste, Italy
[61] Inha University, Incheon, Republic of Korea
[62] Institute for Gravitational and Subatomic Physics (GRASP), Utrecht University/Nikhef, Utrecht, Netherlands

[63] Institute for Nuclear Research, Academy of Sciences, Moscow, Russia
[64] Institute of Experimental Physics, Slovak Academy of Sciences, Košice, Slovakia
[65] Institute of Physics, Homi Bhabha National Institute, Bhubaneswar, India
[66] Institute of Physics of the Czech Academy of Sciences, Prague, Czech Republic
[67] Institute of Space Science (ISS), Bucharest, Romania
[68] Institut für Kernphysik, Johann Wolfgang Goethe-Universität Frankfurt, Frankfurt, Germany
[69] Instituto de Ciencias Nucleares, Universidad Nacional Autónoma de México, Mexico City, Mexico
[70] Instituto de Física, Universidade Federal do Rio Grande do Sul (UFRGS), Porto Alegre, Brazil
[71] Instituto de Física, Universidad Nacional Autónoma de México, Mexico City, Mexico
[72] iThemba LABS, National Research Foundation, Somerset West, South Africa
[73] Jeonbuk National University, Jeonju, Republic of Korea
[74] Johann-Wolfgang-Goethe Universität Frankfurt Institut für Informatik, Fachbereich Informatik und Mathematik, Frankfurt, Germany
[75] Joint Institute for Nuclear Research (JINR), Dubna, Russia
[76] Korea Institute of Science and Technology Information, Daejeon, Republic of Korea
[77] KTO Karatay University, Konya, Turkey
[78] Laboratoire de Physique des 2 Infinis, Irène Joliot-Curie, Orsay, France
[79] Laboratoire de Physique Subatomique et de Cosmologie, Université Grenoble-Alpes, CNRS-IN2P3, Grenoble, France
[80] Lawrence Berkeley National Laboratory, Berkeley, California, United States
[81] Lund University Department of Physics, Division of Particle Physics, Lund, Sweden
[82] Moscow Institute for Physics and Technology, Moscow, Russia
[83] Nagasaki Institute of Applied Science, Nagasaki, Japan
[84] Nara Women's University (NWU), Nara, Japan
[85] National and Kapodistrian University of Athens, School of Science, Department of Physics , Athens, Greece
[86] National Centre for Nuclear Research, Warsaw, Poland
[87] National Institute of Science Education and Research, Homi Bhabha National Institute, Jatni, India
[88] National Nuclear Research Center, Baku, Azerbaijan
[89] National Research Centre Kurchatov Institute, Moscow, Russia
[90] Niels Bohr Institute, University of Copenhagen, Copenhagen, Denmark
[91] Nikhef, National institute for subatomic physics, Amsterdam, Netherlands
[92] NRC Kurchatov Institute IHEP, Protvino, Russia
[93] NRC «Kurchatov»Institute - ITEP, Moscow, Russia
[94] NRNU Moscow Engineering Physics Institute, Moscow, Russia
[95] Nuclear Physics Group, STFC Daresbury Laboratory, Daresbury, United Kingdom
[96] Nuclear Physics Institute of the Czech Academy of Sciences, Řež u Prahy, Czech Republic
[97] Oak Ridge National Laboratory, Oak Ridge, Tennessee, United States
[98] Ohio State University, Columbus, Ohio, United States
[99] Petersburg Nuclear Physics Institute, Gatchina, Russia
[100] Physics department, Faculty of science, University of Zagreb, Zagreb, Croatia
[101] Physics Department, Panjab University, Chandigarh, India
[102] Physics Department, University of Jammu, Jammu, India
[103] Physics Department, University of Rajasthan, Jaipur, India
[104] Physikalisches Institut, Eberhard-Karls-Universität Tübingen, Tübingen, Germany
[105] Physikalisches Institut, Ruprecht-Karls-Universität Heidelberg, Heidelberg, Germany
[106] Physik Department, Technische Universität München, Munich, Germany
[107] Politecnico di Bari and Sezione INFN, Bari, Italy
[108] Research Division and ExtreMe Matter Institute EMMI, GSI Helmholtzzentrum für Schwerionenforschung GmbH, Darmstadt, Germany

[109] Rudjer Bošković Institute, Zagreb, Croatia
[110] Russian Federal Nuclear Center (VNIIEF), Sarov, Russia
[111] Saha Institute of Nuclear Physics, Homi Bhabha National Institute, Kolkata, India
[112] School of Physics and Astronomy, University of Birmingham, Birmingham, United Kingdom
[113] Sección Física, Departamento de Ciencias, Pontificia Universidad Católica del Perú, Lima, Peru
[114] St. Petersburg State University, St. Petersburg, Russia
[115] Stefan Meyer Institut für Subatomare Physik (SMI), Vienna, Austria
[116] SUBATECH, IMT Atlantique, Université de Nantes, CNRS-IN2P3, Nantes, France
[117] Suranaree University of Technology, Nakhon Ratchasima, Thailand
[118] Technical University of Košice, Košice, Slovakia
[119] The Henryk Niewodniczanski Institute of Nuclear Physics, Polish Academy of Sciences, Cracow, Poland
[120] The University of Texas at Austin, Austin, Texas, United States
[121] Universidad Autónoma de Sinaloa, Culiacán, Mexico
[122] Universidade de São Paulo (USP), São Paulo, Brazil
[123] Universidade Estadual de Campinas (UNICAMP), Campinas, Brazil
[124] Universidade Federal do ABC, Santo Andre, Brazil
[125] University of Cape Town, Cape Town, South Africa
[126] University of Houston, Houston, Texas, United States
[127] University of Jyväskylä, Jyväskylä, Finland
[128] University of Liverpool, Liverpool, United Kingdom
[129] University of Science and Technology of China, Hefei, China
[130] University of South-Eastern Norway, Tonsberg, Norway
[131] University of Tennessee, Knoxville, Tennessee, United States
[132] University of the Witwatersrand, Johannesburg, South Africa
[133] University of Tokyo, Tokyo, Japan
[134] University of Tsukuba, Tsukuba, Japan
[135] Université Clermont Auvergne, CNRS/IN2P3, LPC, Clermont-Ferrand, France
[136] Université de Lyon, Université Lyon 1, CNRS/IN2P3, IPN-Lyon, Villeurbanne, Lyon, France
[137] Université de Strasbourg, CNRS, IPHC UMR 7178, F-67000 Strasbourg, France, Strasbourg, France
[138] Université Paris-Saclay Centre d'Etudes de Saclay (CEA), IRFU, Départment de Physique Nucléaire (DPhN), Saclay, France
[139] Università degli Studi di Foggia, Foggia, Italy
[140] Università degli Studi di Pavia and Sezione INFN, Pavia, Italy
[141] Università di Brescia and Sezione INFN, Brescia, Italy
[142] Variable Energy Cyclotron Centre, Homi Bhabha National Institute, Kolkata, India
[143] Warsaw University of Technology, Warsaw, Poland
[144] Wayne State University, Detroit, Michigan, United States
[145] Westfälische Wilhelms-Universität Münster, Institut für Kernphysik, Münster, Germany
[146] Wigner Research Centre for Physics, Budapest, Hungary
[147] Yale University, New Haven, Connecticut, United States
[148] Yonsei University, Seoul, Republic of Korea